Pre-collisional crustal evolution of the European Variscan periphery: constraints from detrital zircon U–Pb ages and Hf isotopic record in the Precambrian metasedimentary basement of the Brunovistulian Domain

Igor Soejono[a*], Karel Schulmann[a], Jiří Sláma[b], Kristýna Hrdličková[a], Pavel Hanžl[a], Jiří Konopásek[a, c], Stephen Collett[a], Jitka Míková[a]

[a] *Czech Geological Survey, Klárov 3, 118 21 Prague 1, Czech Republic*

[b] *Institute of Geology of the CAS, v. v. i., Rozvojová 269, 165 00 Prague 6, Czech Republic*

[c] *Department of Geosciences, UiT The Arctic University of Norway, Dramsveien 201, 9037 Tromsø, Norway*

**Corresponding author (e-mail: igor.soejono@geology.cz, telephone: (+420) 257089497, fax: (+420) 257531376*

Abstract

In this study, U–Pb ages and Hf isotopic composition of detrital zircons from the Precambrian metasedimentary autochthon of the Brunovistulian Domain in the eastern Bohemian Massif were investigated to understand the pre-collisional evolution of the eastern periphery of the European Variscan belt. Detrital zircons of the Tonian sequences have mostly Paleoproterozoic to Neoproterozoic ages (c. 2.1–0.9 Ga) and are interpreted as detritus derived from the basement of either Baltica or Amazonia. The mostly positive $\varepsilon_{Hf(t)}$ values (–4 to +16) indicate a juvenile nature of their magma sources with minor older crustal components. In contrast, the Ediacaran sequences contain dominantly Neoproterozoic zircons (c. 600 Ma) and only rare Paleo- and Mesoproterozoic ages indicate that they were sourced from the adjacent Neoproterozoic magmatic arc with very limited input of recycled cratonic detritus. The large spread of $\varepsilon_{Hf(t)}$ values (–15 to +13) of the Neoproterozoic zircons suggests significant mixing of mantle-derived magmas with mature crustal material, typical of large continental magmatic arc systems. The zircon age patterns of the Ediacaran sequences, characterized by a dominance of the late Neoproterozoic zircons and limited Mesoproterozoic zircons, are nearly identical to those from the Teplá–Barrandian Unit and Moldanubian Zone, pointing to their similar sources. We consider such age populations as a record of sources actually exposed at the time of deposition, rather than the real provenance signature of the continental basement. The change in detrital zircon U–Pb age and Hf record of the Brunovistulian Domain took place between the early and late Neoproteorozoic, and probably reflects the plate-tectonic reconfiguration from the Rodinia formation/break-up to the evolution of the Gondwana or Baltica active margins. Our data challenge the main arguments for an existence of the Rheic oceanic suture between the Brunovistulian Domain and

Moldanubian Zone and allow for an alternative pre-collisional model of the Bohemian Massif as a single Neoproterozoic crustal domain.

Keywords: Detrital zircon dating, Hf isotopes, Brunovistulian Domain, Bohemian Massif, Paleogeoraphy, Pre-collisional evolution

1. Introduction

The tectonic evolution of the principal crustal domains involved in the European Variscan orogenic system has been studied by many geologists for almost a century (e.g. Franke, 2000; Kossmat, 1927; Matte, 1986; Schulmann et al., 2014a; Winchester, 2002). Despite a significant progress in our understanding of late Paleozoic tectono-metamorphic processes related to the amalgamation of the Pangea supercontinent (e.g. Edel et al., 2018; Martínez Catalán et al., 2020), the pre-collisional evolution of these domains remains controversial. In particular, their paleogeographic position within the Rodinia and Gondwana supercontinents is largely unresolved, as well as their relationship to the Proterozoic and early Paleozoic oceanic domains. Specifically, it is uncertain whether the individual crustal domains were derived from Baltica, or whether they were adjacent to Amazonian or African parts of the northern Gondwana margin (e.g. Henderson et al., 2016; Samson et al., 2005; von Raumer et al., 2002). Resolving such questions can contribute to our understanding of not only the pre-orogenic history of the principal crustal segments forming the European Variscan belt, but also their subsequent collisional evolution.

The Brunovistulian Domain or Brunovistulicum, as one of the most ancient continental blocks incorporated in the eastern part of the Variscan orogenic belt (Fig. 1a) represents a key area for understanding the missing elements of the pre-orogenic history of the Bohemian Massif. While the late Proterozoic magmatic evolution of the Brunovistulian continental arc system is relatively well-established (Finger et al., 2000a; Hanžl et al., 2019; Soejono et al., 2017), its Precambrian paleogeographic position is widely discussed. The two most common scenarios suggest that the Brunovistulian Domain was originally derived from Baltica (Belka et al., 2002; Dudek, 1980; Nawrocki et al., 2004; Vavrdová et al., 2003; Żelaźniewicz et al., 2020) or from the Avalonian (Amazonian) part of the northern Gondwana margin (Finger et al., 2000a; Friedl et al., 2000; Jastrzębski et al., 2021; Lindner et al., 2020; Mazur et al., 2010; Moczydłowska, 1997). The second model is based mainly on the presence of Mesoproterozoic (1.6–1.0 Ga) xenocrysts and inherited zircon cores in orthogneiss from the allochthonous Moravo–Silesian Zone (Fig. 1) firstly reported by Friedl et al. (2000). These are typically interpreted to have been sourced from magmatic complexes widespread in the Amazonian Craton (Cardona et al., 2009; Cordani and Teixeira, 2007; McLelland et al., 2010; Nance and Murphy, 1994). Such a zircon age pattern was later confirmed in other meta-igneous rocks across the whole Moravo–Silesian Zone (Friedl et al., 2004; Klimas et al., 2009; Lindner et al., 2020; Mazur et al., 2010; Oberc-Dziedzic et al., 2003; Soejono et al., 2017). However, these old inherited zircons were so far undetected within the Brunovistulian autochthon.

In general, an abundance of inherited zircons is typical mainly of crustal-derived S-type granites whereas it is rare in hotter and less siliceous I-type magmas (Binderman and Melnik, 2016; Miller et al., 2003; Janoušek et al., 2006; Watson and Harrison, 1983). Therefore, U–Pb detrital zircon dating is a significantly more reliable tool for tracing clastic sources and crustal provenance. It allows correlation of different continental domains and studies of sedimentary processes related to their amalgamation (Cawood et al., 2012; Dickinson and Gehrels, 2009; Fedo et al., 2003; Gehrels, 2014; Lancaster et al., 2011; Stephan et al., 2019; Žák et al., 2020). The study of in-zircon Hf isotopic signatures coupled with U–Pb dating is another important method to determine the nature of the magmatic sources of detrital zircon, as it provides information about isotopic evolution of the source crust (e.g. Belousova et al., 2010; Hawkesworth and Kemp, 2006; Lancaster et al., 2011).

In the Bohemian Massif, detrital zircon age populations have been recently studied in the Saxothuringian Zone (Collett et al., 2020; Linnemann et al., 2014; Tabaud et al., 2021;

Žáčková et al., 2012), Teplá–Barrandian Unit (Drost et al., 2011; Hajná et al., 2018) and Moldanubian Zone (Košler et al., 2014; Pertoldová et al., 2014; Soejono et al., 2020; Žák and Sláma, 2018). Detrital zircon ages from the Brunovistulian Domain have so far only been investigated in the metasedimentary nappes of the Moravo–Silesian Zone (Jastrzębski et al., 2021; Košler et al., 2014) and lower Cambrian sandstones of the Upper Silesia Block in the northern Slavkov Terrane (Habryn et al., 2020; Żelaźniewicz et al., 2020). On the other hand, a detailed provenance study has not yet been conducted for the main part of the Precambrian Brunovistulian basement, despite the presence of sufficiently old rocks (e.g. Collett et al., 2021) that can potentially bear information about the sources of clastic material available at the time of their formation.

To fill this gap, we conducted a geochronological study of detrital U–Pb zircon grains and their Hf isotopic compositions from Precambrian metasediments of the Brunovistulian basement and surrounding units. The data enable estimation the depositional age, and discussion of tectonic setting and possible crustal source regions, which can be deduced from comparison with similar datasets from the adjacent parts of the Bohemian Massif. Finally, possible Neoproterozoic paleogeographic models are discussed and a new pre-collisional scenario for this poorly known part of the European Variscan belt is proposed.

2. Geological setting of the Brunovistulian Domain

The Brunovistulian Domain is exposed at the eastern margin of the Bohemian Massif (Fig. 1b) and represents a fragment of the Precambrian continental crust located between the Variscan collisional system in the west, the Carpathian belt to the southeast and

East European Craton to the north (Dudek, 1980; Mazur et al., 2015, 2018). The western Brunovistulian margin is reworked by a 50 km wide and 300 km long Moravo–Silesian Zone represented by imbricated and metamorphosed nappes (Suess, 1912, 1926). This zone is considered as a main tectonic boundary between the Moldanubian Zone composed of high-grade gneisses, migmatites, granulites and various intrusive rocks, and the Brunovistulian promontory further east (Schulmann et al., 2008; Štípská et al., 2008). Carboniferous thrusting-related exhumation of the Moldanubian Zone over the Brunovistulian basement (Racek et al., 2017; Štípská et al., 2020) resulted in the development of an up to 7 km thick Carboniferous Culm foreland basin unconformably covering the Precambrian basement and its early Paleozoic cover. In the southeast, the Brunovistulian Domain is overthrust by the Cretaceous–Paleogene nappes of the Outer Western Carpathians (Dudek, 1980; Šamajová et al., 2018).

Despite significant progress during the last decades, the primary pre-collisional relationship of the Brunovistulian Domainand the Moldanubian Zone remains controversial. Many authors have considered their mutual boundary as a continuation of the Rheic suture from the northwestern Europe (e.g. Finger et al., 1998; Höck et al., 1997; Jastrzębski et al., 2013). However, this mainstream idea was challenged by Schulmann et al. (2005, 2009, 2014b) who suggested that the Moldanubian Zone originally represented an early Paleozoic basin formed above a stretched Brunovistulian margin and that these two units were not separated by an extensive ocean. The pre-Variscan evolution of the Brunovistulian Domain has been mainly associated with the Cadomian Orogeny (Dudek, 1980; Finger et al., 2000a; Hanžl and Melichar, 1997; Jelínek and Dudek, 1993; Kröner et al., 2000) at c. 650–550 Ma (Linnemann et al., 2014; Nance and Murphy, 1994; Nance et al., 1991). Later studies revealed a multi-stage Neoproterozoic magmatic evolution associated with long-lived active margin, operating in the c. 730–570 Ma period (Hanžl et al., 2019; Soejono et al., 2017). Noticeably, numerous fragments of Precambrian rocks such as c. 1370 Ma Mesoproterozoic granitoids, early Neoproterozoic sedimentary rocks and late Neoproterozoic c. 576 Ma magmatic arc granitoids were reported from the Moldanubian Zone as well (Friedl et al., 2004; Lindner et al., 2018, 2020, 2021) and consequently considered to be the western continuation of the Brunovistulian basement.

2.1. Subdivision, lithology and age

The Brunovistulian Domain has been divided into three main zones (Finger et al., 1995; Suess, 1912): the western Moravo–Silesian Zone, the Thaya Terrane in the middle and the Slavkov Terrane to the east (Fig. 1). The term “terrane” is used here in the sense of regional lithotectonic unit with partially different lithologies and/or age.

The Moravo–Silesian Zone forms a NE–SW trending belt of orthogneisses and metasedimentary thrust sheets emerging through the rocks of the Moldanubian Zone in a form of three tectonic windows forming the so-called Moravian Zone in the south and the Silesian Zone in the north (Suess, 1912; 1926). In Poland, the Moravo–Silesian Zone crops out in the Fore-Sudetic block (Mazur et al., 2010; Oberc-Dziedzic et al., 2003). The hanging-wall Moldanubian Zone is separated from the Moravian foot-wall by the so-called Micaschist Zone (Suess, 1912) and the early Cambrian Letovice mafic complex (Soejono et al., 2010, Fig. 1). Orthogneiss protoliths of the Moravo–Silesian Zone, derived from a highly evolved crustal source, represent the most mature members of arc-related granitoids in the Brunovistulian Domain (Finger et al., 2000a; Mazur et al., 2010; Soejono et al., 2017). Their U–Pb magmatic ages are in the interval of 586–578 Ma (Friedl et al., 2000; Kröner et al., 2000; Soejono et al., 2017). In the Fore-Sudetic Block, the protoliths of orthogneisses were dated at 602–557 Ma (Klimas et al., 2009; Mazur et al., 2010; Oberc-Dziedzic et al., 2003, 2021).

The Thaya Terrane crops out in the western part of the Brno Massif and the Thaya Massif and represents the para-autochthon of the Moravian nappes (Schulmann et al., 1991; Soejono et al., 2017). The eastern part of the Thaya Terrane in the footwall of the Moravian Zone consists mainly of deformed biotite granodiorite to granite (Finger et al., 1995, 2000a). In the west, the Thaya Terrane is dominated by granodiorites showing intrusive contacts with weakly metamorphosed gabbros, quartz diorites and tonalites of the Metadiorite Zone in the east (Hanžl et al., 2019; Jelínek and Dudek, 1993). Characteristic feature of the Thaya Terrane is a large number of metamorphosed volcanosedimentary host-rock xenoliths interpreted as roof pendants of the main granodiorite intrusion (Hanžl et al., 2019). Igneous rocks of the Thaya Terrane were interpreted as relatively evolved I-type magmas generated by melting of continental crust in an Andean-type magmatic arc environment (Finger et al., 2000a; Hanžl and Melichar, 1997; Hanžl et al., 2019; Soejono et al., 2017). Available geochronological data show that the granodiorites of the Thaya Terrane intruded between 634–567 Ma with a peak of magmatism at c. 600 Ma (Soejono et al., 2017; Svojtka et al., 2017; Van Breemen et al., 1982), whereas diorites and tonalites of the Metadiorite Zone formed at c. 650 Ma (Hanžl et al., 2019).

The Metabasite Zone is a N–S trending narrow belt in the central part of the Brno Massif, separating the Slavkov and Thaya terranes. It consists of low-grade metabasalts intercalated with layers of metarhyolites (Finger et al., 2000b; Hanžl et al., 2019) which were interpreted as a relic of oceanic crust (Finger et al., 2000a; Hanžl and Melichar, 1997) or a fragment of a back-arc or forearc basin (Hanžl et al., 2019). The rhyolites were dated at c. 730 Ma by Pb–Pb zircon evaporation method (Finger et al., 2000b) and by LA–ICP–MS U–Pb dating of zircon (Hanžl et al., 2019; Timmerman et al., 2019) and represent thus the oldest rocks of the Brunovistulian Domain.

The exposed outcrops of the Slavkov Terrane are represented mainly by granodiorites and their metasedimentary host rocks of the eastern Brno Massif (Finger et al., 2000a; Hanžl and Melichar, 1997; Jelínek and Dudek, 1993), and metagranites and orthogneisses cropping out in the para-autochthon of the Silesian Zone (Hanžl et al., 2007; Kröner et al., 2000). The granodiorites of the eastern Brno Massif have been dated at c. 586 Ma by Ar^{40}–Ar^{39} method (amphibole cooling ages; Fritz et al., 1996) and at c. 595 Ma by zircon U–Pb method (Timmerman et al., 2019), and interpreted as primitive I-type granitoids formed in an island-arc setting (Finger et al., 2000a; Jelínek and Dudek, 1993). Boreholes reached mainly metasedimentary rocks and metabasites beneath the sedimentary cover of the northern parts of the Slavkov Terrane (Dudek, 1980; Jelínek and Dudek, 1993; Żelaźniewicz et al., 2009), but locally also fragments of the Neoarchean and Paleoproterozoic basement (Żelaźniewicz and Fanning, 2020).

The Brunovistulian Precambrian crystalline basement is unconformably overlain by the late Proterozoic and Paleozoic sedimentary cover (Dudek, 1980; Kalvoda et al., 2008). It is composed of Ediacaran low-grade turbiditic and deltaic siliciclastic rocks at the base (Buła and Jachowitz, 1996; Moczydlowska, 1997; Nawrocki et al., 2004; Vavrdová et al., 2003; Żelaźniewicz et al., 2009, 2020) and Ordovician–Silurian marine strata, which are exotic in the southern part (Kettner and Remes, 1936). The sequence continues with the Lower–Middle Devonian platform-type continental clastic sediments and limestones (Chlupáč, 1989; Kalvoda et al., 2008) and Upper Devonian to Lower Carboniferous volcano-sedimentary back-arc basin sequences (Hladil et al., 1999; Janoušek et al., 2014). The Devonian sequences are in the east covered by the lower Carboniferous Variscan foreland basin (Hartley and Otava, 2001; Tomek et al., 2019), which pass to the upper Carboniferous continental mollase further east (Kalvoda et al., 2008; Špaček and Kalvoda, 2000).

3. Methods

Zircon grains were separated using conventional methods (crushing, Wilfley concentration table, magnetic and heavy liquid separations) from c. 15 kg of rock per outcrop sample and c.

1.5 kg per drill-core sample. The zircon U–Pb dating followed closely the technique described in detail in Soejono et al. (2020). The laser was fired at a repetition rate of 5 Hz and fluence of 4.4 J/cm^2 with 22 micron spot size. The carrier gas was flushed through the two-volume ablation cell at a flow rate of 0.9 l/min and mixed with 0.66 l/min Ar and 0.003 l/min N_2 prior to introduction into the ICP. Residual elemental fractionation and instrumental mass bias were corrected by normalization of internal natural zircon reference material 91500 (Wiedenbeck et al., 1995). Zircon reference materials GJ-1 (Jackson et al., 2004) and Plešovice (Sláma et al., 2008b) were periodically analysed during the measurement for quality control. The obtained values (near-concordant GJ-1: mean Concordia age of 602 ± 3 Ma (2σ); near-concordant Plešovice: mean Concordia age of 340 ± 2 (2σ)) fit well and are less than 1 % off their published reference values (GJ-1: 600.5 ± 0.4 Ma (Schaltegger et al., 2015); Plešovice: 337.1 ± 0.4 Ma, (Sláma et al., 2008b). The zircon U–Pb ages are presented as a concordia diagrams generated with the ISOPLOT program v. 3.70 (Ludwig, 2008), and histograms with a kernel density estimate (Andersen et al., 2017). Only analyses less than 10 % discordant were taken into account. For the data interpretation, the ^{207}Pb/^{206}Pb age was used for zircons older than 1 Ga, while the ^{206}Pb/^{238}U age was used for zircons younger than 1 Ga.

Maximum depositional ages (MDA) were calculated using the 2–5 youngest zircons following Dickinson and Gehrels (2009). These are presented as concordia ages calculated from the youngest zircons overlapping in age at 1σ and with <2% discordance or as the weighted mean ages.

Hf isotopes were analysed using the Photon Machines Analyte Excite 193 nm excimer laser system equipped with a two-volume HelEx ablation cell that was connected to the Thermo-Finnigan Neptune MC ICP-MS instrument equipped with an array of eight movable

Faraday collectors (L4, L3, L2, L1, H1, H2, H3, H4) and one fixed center collector (C). All the measurements were performed in a static multi-collection and low mass resolution mode. Samples were ablated in He atmosphere (0.8 l min^{-1}), the laser was fired with energy of 9.42 J/cm^2, laser beam diameter was 40 μm and repetition rate was 10 Hz. Each measurement consisted of 20 s of blank acquisition followed by ablation of the sample for further 40 s. The faraday cup configuration was set to enable detection of all Hf isotopes as well as potentially interfering ions: L4 – ^{171}Yb, L3 – ^{173}Yb, L2 – ^{175}Lu, L1 – ^{176}Hf, C – ^{177}Hf, H1 – ^{178}Hf, H2 – ^{179}Hf, H3 – ^{180}Hf. Data were corrected for gas blank and isobaric interferences of Yb and Lu on ^{176}Hf using the signals of the interference-free isotopes ^{171}Yb, ^{173}Yb and ^{175}Lu monitored during the analyses. The ^{176}Yb and ^{176}Lu contribution was calculated using the isotopic abundance of Lu and Hf proposed by Chu et al. (2002). The measurements of ^{171}Yb and ^{173}Yb permit to correct the mass bias fractionation of Yb using a $^{173}Yb/^{171}Yb$ normalization factor of 1.132685 (Chu et al. 2002). Instrumental mass bias for Hf was corrected based on the measured ^{179}Hf and ^{177}Hf intensities and the natural ratio ($^{179}Hf/^{177}Hf$ = 0.7325) using the exponential law (Chu et al., 2002). As a monitor of data quality 91500 natural zircon reference samples 91500 (Wiedenbeck et al., 1995), GJ-1 (Jackson et al., 2004) and Plešovice (Sláma et al., 2008b) were periodically measured between sample analyses. Multiple laser ablation MC ICP-MS analyses of the reference zircons 91500, GJ-1 and Plešovice yielded a $^{176}Hf/^{177}Hf$ ratio of 0.2822913±0.0000091 (2σ), 0.282018±0.000016 (2σ) and 0.282482±0.0000044 (2σ), respectively.

The values used to calculate the Hf isotopic data were: chondritic uniform reservoir (CHUR): $^{176}Lu/^{177}Hf$ = 0.0332, $^{176}Hf/^{177}Hf$ = 0.282772 (BlichertToft and Albarede, 1997); Depleted Mantle (DM): $^{176}Lu/^{177}Hf$ = 0.0384, $^{176}Hf/^{177}Hf$ = 0.28325 (Chauvel and Blichert-Toft, 2001); continental crust: $^{176}Lu/^{177}Hf$ = 0.0113 (Zeh et al., 2007); ^{176}Lu decay constant =

1.8648×10^{-11} (Scherer et al., 2001). The single-stage Hf model ages (T_{DM}) were taken for zircons with positive $\varepsilon_{Hf(t)}$ values and two-stage Hf model ages (T_{DM2}) for negative $\varepsilon_{Hf(t)}$ values. U–Pb, Hf isotopic data as well as Th/U ratios for each sample are listed in the electronic supplementary material B.

4. Results

4.1. Samples

In this study, eleven high-grade metasedimentary rocks were studied to cover all of the main units of the Brunovistulian Domain (Fig. 1; Table 1), including five samples from outcrops and six from the drill-cores drilled during the 1970s for oil exploration (Dudek, 1980). Based on combined regional position, maximum depositional age and similarities in detrital zircon age spectra, the studied metasedimentary samples were divided into four groups: 1) **Tonian pre-Cadomian successions** of the Thaya Terrane represented by two samples of host-rock of the western Brno Massif, 2) one sample from the eastern Slavkov Terrane and six borehole core samples from the covered part of the Brunovistulian Domain representing **the Ediacaran synorogenic sequences**, 3) **Moravo–Silesian Zone** and 4) **Micaschist Zone** represented by one sample each. The positions and characteristics of the samples are provided in the Table 1 and photographs of all studied samples are shown in Supplementary material A.

The host-rock of the western Brno Massif, represented by the two studied samples (Fig. 1) is intruded by granodiorite apophyses (Fig. 2a, b) dated at 601 ± 3 Ma (Soejono et al., 2017). Sample UD 16 is a fine-grained migmatized paragneiss dominantly composed of feldspars, biotite, quartz and garnet (Fig. 3a) with minor tourmaline and accessory apatite and zircon. Sample UD 23 is a stromatic fine-grained migmatite composed of alternating quartz-feldspathic leucosome and restite bands. Restite consists mainly of biotite, garnet and pseudomorphs after cordierite composed of biotite, chlorite, rare muscovite, feldspar and quartz (Fig. 3b). The main accessories are apatite and zircon.

Migmatized paragneiss UD 18, taken from the para-autochthon of the Silesian Zone at the NW margin of the Slavkov Terrane (Fig.1), includes quartz, biotite, muscovite, plagioclase and accessory apatite and zircon. Sample UD 30 is amphibole-biotite gneiss from a depth of 3095 m of the Strachotín 2 borehole in the Thaya Terrane (Fig.1). Massive fine- to medium-grained amphibole-biotite gneiss is composed of prevailing plagioclase, amphibole and biotite. K-feldspar and quartz are also present in negligible amounts and apatite, zircon and pyrite are accessory. Sample UD 31 is a fine-grained migmatized paragneiss from 1459 m depth of the Bystřice 1 borehole in the northeastern part of the Slavkov Terrane (Fig.1). The sample is a paragneiss characterized by alternating quartz-feldspar and garnet-biotite bands. Main accessories are zircon and apatite concentrated in quartz-feldspar bands. Fine-grained paragneiss sample UD 32 comes from 4000 m depth of the Slušovice 1 borehole in the central part of the Slavkov Terrane (Fig.1). Mineral assemblage consists of chloritized biotite, quartz, feldspars (albite–oligoclase), muscovite and garnet. Sample UD 33 is a sillimanite-biotite paragneiss from the 1562 m depth of the borehole Krásná NP823 in the northeastern Slavkov Terrane (Fig. 1, 3c). Its mineral assemblage consists of quartz, feldspars and biotite locally accompanied by fibrous sillimanite and garnet. Muscovite is present in the form of relatively rare lathes concentrated in biotite-rich bands. Accessory phases are tourmaline, zircon and apatite. Sample UD 34 is a fine-grained migmatized paragneiss from 3248 m depth of the Mi 1 borehole in the southwestern part of the Slavkov Terrane (Fig.1). The rock is locally migmatized and injected by granitic melt parallel to the foliation. The mineral association comprises K-feldspar and plagioclase (oligoclase to andesine), quartz, biotite, minor muscovite, secondary chlorite and accessory zircon. Sample of medium-grained amphibole-biotite paragneiss UD 35 was taken from the 2274 m depth of the Krásná 1 borehole in the northeastern part of the Slavkov Terrane (Fig. 1, 3d). This rock is composed mainly of quartz, feldspar, biotite and amphibole.

Sample UD 11, taken from the lowermost metasedimentary nappe of the Svratka Dome in the central part of the Moravo–Silesian Zone (Fig. 1), is a banded quarzitic schist (Fig. 2e) marked by alternation of fine and medium grained bands accented by dark (fine grained, with Fe oxides) and light (medium grained) colours (Fig. 3e). It is dominantly composed of quartz with subordinate feldspar, biotite and muscovite. Apatite and zircon are present as accessories. Medium-grained micaschist sample UD 20 represents the northern part of the Micaschist Zone north of the Svratka Dome (Fig. 1). This medium-grade garnet micaschist of the kyanite zone (Fig. 2f) consists mainly of muscovite and biotite aggregates alternating with quartz layers and up to 3 mm large garnet porphyroblasts and accessory apatite, zircon and opaque minerals (Fig. 3f).

4.2. U–Pb detrital zircon dating and Hf isotopic signatures

4.2.1. Tonian sequences

Zircon grains from the sample UD 16 are mostly 40–100 µm long, generally shortly prismatic with rounded or sub-rounded crystal shapes. Most of the grains show truncated oscillatory zoning (Fig. 4a). Some zircons have older corroded cores overgrown by zoned or unzoned rims. U–Pb zircon dating (100 analyses) yielded a wide spectrum of ages, with a few youngest ages between c. 950 and 898 Ma, a broad major peak between c.1.0 and 2.2 Ga and a few outliers around 2.7 Ga (Fig. 5a). Three younger ages at c. 740, 600 and 380 Ma (not shown on the Fig. 4a but listed in Supplementary material B) are interpreted as related to the metamorphic resetting or metamictization. The maximum depositional age calculated for this sample is 912 ± 17 Ma (Fig. 6a). Twenty-seven grains were analysed for Hf isotopic composition. Meso- and Paleoproterozoic zircons have mostly positive $\varepsilon_{Hf(t)}$ values mostly ranging from –1 to +16 and Hf model ages between 2.4 and 1.3 Ga. Few zircon grains show slightly negative $\varepsilon_{Hf(t)}$ values (Fig. 7a), with Hf model ages between 2.9 and 2.3 Ga.

Sample UD 23 contains c. 30–80 μm long and mostly rounded zircons with oscillatory zoning and dark rims (Fig. 4b). The age population of sample UD 23 is very similar to that of sample UD 16. A total of 68 analyses show a dominant wide age cluster between c. 1.9 and 0.9 Ga and few data around 2.6 Ga (Fig. 5b). One outlier at c. 800 Ma was detected in a zircon of noticeably different morphology (euhedral prismatic grain with bright CL signal). Due to the high risk of contamination, this zircon grain was excluded (not shown on the Fig. 4b but listed in Supplementary material A). The maximum depositional age of sample UD 23 is 949 ± 79 Ma (Fig. 6b).

4.2.2. Ediacaran sequences

Zircons extracted from paragneiss UD 18 are c. 80–150 μm long, stubby or short-prismatic. They generally have well-preserved crystal faces with oscillatory or sector zoning (Fig. 4c). LA–ICP–MS zircon dating (112 analyses) provided a major age peak at c. 650 Ma and a broad subordinate cluster between c. 2.5 and 1.8 Ga (Fig. 5c). The maximum depositional age is 604 ± 7 Ma (2σ; Fig. 6c).

Zircon grains from sample UD 30 have generally stubby or long-prismatic and euhedral shapes with a length of 60–200 μm. They are oscillatory or sector zoned with common thin dark or bright overgrowths. Some grains also show irregular convolute zoning in their internal part (Fig. 4d). The age spectrum of sample UD 30 (86 analyses) has a clear unimodal distribution with a single age group around c. 640 Ma (Fig. 5d). U–Pb dating also yielded few data between c. 515 and 300 Ma (not shown in the diagram) considered as a result of Pb-loss and/or probable contamination in the case of the youngest date(s). The maximum depositional age calculated for this sample is 579 ± 5 Ma (Fig. 6d). Twenty three grains of Neoproterozoic age show a wide range of $\varepsilon_{Hf(t)}$ values from –15 to +13 (Fig. 7b), with systematic negative correlation between the Hf model ages (2.2–0.65 Ga) and $\varepsilon_{Hf(t)}$ values.

Paragneiss UD 31 contains 50–120 μm long euhedral or subhedral isometric, shortly prismatic and fragmented zircon grains. Internal structures of zircons exhibit mostly oscillatory or sector zoning and rare rounded distinct cores (Fig. 4e). The zircon age population (79 analyses) is nearly identical as that of previous sample UD 30 with the main peak at c. 620 Ma and single ages at c. 1.0 and 2.9 Ga (Fig. 5e). Besides, nine grains with younger ages (c. 544–467 Ma; not shown in Fig. 5e) have somewhat lower CL intensity, and higher contents of U than older zircons and higher discordance. These data are considered as related to Pb-loss, possibly during extensive anatexis. The maximum depositional age is 596 ± 7 Ma (Fig. 6e).

Sample UD 32 contains mostly euhedral and shortly-prismatic zircon grains with lengths of 30–120 μm mostly with clear oscillatory zoning (Fig. 4f). U–Pb zircon dating of this sample (92 analyses) yielded wide range of ages with the dominant peak at c. 630 Ma and two minor clusters in intervals of c. 2.2–1.7 Ga and 1.5–1.2 Ga (Fig. 5f). Presence of one single age at c. 490 Ma (not shown) is most likely caused by contamination. The maximum depositional age of sample UD 32 is 602 ± 3 Ma (Fig. 6f).

Zircon population from sample UD 33 contains 80–140 μm long, euhedral to subhedral, shortly-prismatic and stubby grains. Cathodoluminescence internal patterns mostly show oscillatory zoned or rarely unzoned grains with thin dark rims (Fig. 4g). The age spectrum of sample UD 33 (82 analyses) is more varied than in samples from other borehole cores. It has the same main peak at c. 620 Ma, but is significantly richer in older ages in the interval between c. 800 Ma and 2.2 Ga (Fig. 5g). Eight analyses that provided younger ages (c. 555–

495 Ma; not shown) are represented mostly by zircon with higher content of U, low CL and most probably correspond to Pb-loss during Cadomian metamorphism. The maximum depositional age calculated for this sample is 555 ± 4 Ma (Fig. 6g). Meso- to Neoproterozoic zircons (25 grains) have mostly positive $\varepsilon_{Hf(t)}$ values ranging from 0 to +18 (Fig. 7b) with model ages varying from c. 1.6 to 0.75 Ga. One Neoproterozoic outlier shows highly negative $\varepsilon_{Hf(t)}$ value of – 24 corresponding to a two-stage T_{DM2} Hf model age of c. 2.7 Ga.

The majority of zircon grains obtained from sample UD 34 have subhedral and shortly prismatic habit and are 50–100 μm long. They often have oscillatory zoned and sub-rounded internal parts overgrown by relatively thicker, faintly-zoned or unzoned rims (Fig. 4h). Analyses of 84 grains from sample UD 34 yielded age data showing c. 600 Ma youngest age, a major age peak at c. 680 Ma and several individual ages at c. 1.1, 1.6, 1.9 and 2.7 Ga (Fig. 5h). Two ages at c. 514 and 585 Ma could be related to metamorphic resetting. The maximum depositional age of sample UD 34 is 603 ± 5 Ma (Fig. 6h).

Zircons from paragneiss UD 35 are generally stubby and long-prismatic, euhedral and 100–200 μm long and commonly contain sub-rounded zoned and sometimes corroded cores enveloped by thick bright or dark rimes (Fig. 4i). The age population of this sample (91 analyses) resembles that from sample UD 32 with the dominant age group at c. 600 Ma, two minor clusters in intervals of c. 2.1–1.7 Ga and 1.5–1.2 Ga, and a single age at c 2.7 Ga (Fig. 5i). Two analyses younger than c. 553 Ma (c. 530 Ma) do not provide reliable dates; one has extremely low U content resulting in high uncertainty and the other has high U content and thus most probably represents a grain affected by Pb-loss. Significantly higher U content in one c. 425 Ma old zircon indicates higher degree of metamictization. The maximum depositional age calculated for this sample is 555 ± 4 Ma (Fig. 6i). Neoproterozoic zircons (16 grains) and one Archean zircon have a mixed range of $\varepsilon_{Hf(t)}$ values ranging from –5 to

+10 (Fig. 7b). The Hf model ages of Neoproterozoic grains ranging from 2.4 to 0.75 Ga and the Archean zircon has c. 3.3 T_{DM2} Hf model age. One Mezoproterozoic zircon yielded a slightly more positive $\varepsilon_{Hf(t)}$ value of +13.7 corresponding to a T_{DM} model age of c. 1.4 Ga.

4.2.3. Moravo–Silesian Zone

Zircon grains from gneiss UD 11 are mostly subhedral, 80–220 μm long and isometric or shortly-prismatic with either faint oscillatory zoning or unzoned (Fig. 4j). The zircon age population of sample UD 11 (133 analyses) shows a wide range of ages from c. 550 Ma to 3.0 Ga with several nearly equal sub-peaks at c. 560 Ma, 1.0, 1.3, 1.6, 2.2 and 2.6 Ga (Fig. 5j). Five other dates give slightly younger ages (shown in Supplementary material B) and are again interpreted as affected by partial resetting, probably during Variscan metamorphic overprint. The maximum depositional age of sample UD 31 is 550 ± 6 Ma (Fig. 6j). Zircons from the sample UD 11 of Archean to Neoproterozoic age (64 grains) show mixed $\varepsilon_{Hf(t)}$ values ranging from –15 to +12 (Fig. 7c). Their Hf model ages range from c. 3.6 to 0.95 Ga and generally decreasing with higher $\varepsilon_{Hf(t)}$ values. Two Mesoproterozoic grains have a slightly more radiogenic $\varepsilon_{Hf(t)}$ values (c. + 17), with T_{DM} model age of c. 1.4 and 1.2 Ga.

4.2.4. Micaschist Zone

The majority of zircons from the sample UD 20 are 40–150 μm long, shortly- or long-prismatic and subhedral. Cathodoluminescence images exhibit oscillatory or sector internal zoning with sub-rounded and mostly corroded shapes commonly overgrown by a thin bright rim (Fig. 4k). U–Pb zircon dating (129 analyses) revealed an age pattern characterized by a dominant age cluster around c. 600 Ma, two broad minor peaks in the intervals of c. 0.7–1.1 Ga and 1.7–2.4 Ga and few individual ages around c. 2.7 Ga (Fig. 5k). An important feature is a nearly complete lack of Mesoproterozoic zircons in between c. 1.0 and 1.7 Ga. Several younger ages at c. 545–485 Ma are related to a slight Pb-loss, possibly during metamorphic recrystallization. The maximum depositional age calculated for sample UD 20 is 551 ± 6 Ma (Fig. 6k). Analysed zircons from sample UD 20 (47 grains) yielded a complex isotopic pattern clearly containing two distinct groups according age. The first cluster is defined by the Neoproterozoic zircons which have a wide range of $\varepsilon_{Hf(t)}$ values from –27 to +14 (Fig. 7d), corresponding to a Hf model ages varying from c. 2.8 to 0.73 Ga. The second group of the Paleoproterozoic zircons show a significantly narrower range of $\varepsilon_{Hf(t)}$ values from –10 to +11 with model ages between c. 3.3 and 2.0 Ga. One Paleoproterozoic grain has an outlying very negative $\varepsilon_{Hf(t)}$ value of –30 and T_{DM2} Hf model age of c. 4.0 Ga.

5. Discussion

The presented data (Figs. 5, 7) show contrasting zircon age and Hf isotopic patterns of the studied geological units and litostratigraphic sequences. These data are discussed in terms of the timing and tectonic setting of deposition of sedimentary formations. Furthermore, we compare our results with those from other parts of the Bohemian Massif and potential source areas and discuss their pre-collisional relationships and paleogeography.

5.1. Depositional age and tectonic setting

Due to the absence of geochronological data, the protolith age of the metasedimentary complexes of the Brunovistulian Domain has thus far been unconstrained. The calculated maximum depositional ages presented here (Fig. 6) constrain an oldest possible age of deposition. Two host-rocks of the Brno Massif yielded the Tonian age of the youngest zircons (c. 912 Ma for UD 16 and c. 950 Ma for UD 23) while the Ediacaran samples have their maximum depositional ages in the interval between c. 604 and 555 Ma. It is generally accepted that the Brunovistulian Domain, except for its western margin represented by the Moravo–Silesian Zone, has not been significantly affected by Paleozoic deformation and metamorphism (e.g. Dudek, 1980). This is corroborated by the fact that deformed Neoproterozoic sequences are unconformably overlain by lower Cambrian sandstones in the Upper Silesian Block (Buła et al., 2015; Buła and Jachowitz, 1996; Żelaźniewicz et al., 2009). Therefore, the calculated maximum depositional ages for these samples correspond well to the real age of sedimentation. In contrast, the Tonian maximum depositional age of the host-rocks of the Brno Massif could be significantly older than the true depositional age, which is potentially anywhere between the calculated maximum depositional ages and the c. 600 Ma emplacement age of the intruded granodiorite (Soejono et al., 2017).

Revealed depositional ages (youngest at c. 555 Ma) combined with relationship to the overlying lower Cambrian formations imply that the deformation and metamorphism of the Ediacaran sediments took place shortly after their sedimentation. The youngest dated zircons most probably reflect late Cadomian alteration and partial Pb-loss. Only slightly younger ages of c. 550 Ma were previously detected in the metamorphic rocks of the Slavkov Terrane by monazite chemical dating and interpreted as product of contact metamorphism related to mafic magmatism (Finger et al., 1999). However, based on the mostly migmatic nature of the foliation in our studied samples, the Ediacaran sequences underwent HT regional metamorphism. However, the precise timing and conditions of the metamorphic overprint in the Brunovistulian Domain is out of the scope of this paper and need further studies.

Determination of a depositional environment of the studied rocks is problematic due to strong metamorphic overprint and lack of sedimentological and geochemical data. However, zircon shapes and internal structures combined with the distribution of detrital ages and supposed depositional ages allow for at least an approximate determination of the sedimentary tectonic setting (Cawood et al., 2012).

The combined age populations of the Tonian host-rocks of the Brno Massif show a very wide range of ages (Figs. 8b, 9a) and considerable interval between the maximum sedimentary ages and the main age groups (Fig. 8a). Such an age pattern is a result of a relatively long sedimentary transport from the various and mostly old cratonic sources, characteristic of a collisional depositional setting (Cawood et al., 2012). However, due to potentially younger real depositional age than the calculated maximum depositional age, an extensional setting is also possible. Mostly rounded grain shapes and frequently corroded and rimmed cores (Fig. 4a, b) also suggest longer transport and zircon recycling, compatible with both collisional and extensional settings. In our opinion, it is not distinguishable between a syn-collisional and extensional environment for the Tonian basin without any further geological or sedimentological constraints. However, a long time interval between the depositional age and the major zircon age group unequivocally excludes its active margin tectonic setting.

In contrast, all the samples from the Ediacaran sequences (UD 18 and drill-core samples) are dominated by zircons with ages very close to their depositional ages (Fig. 8b), while they do not contain a proportionally significant amount of cratonic detritus (Fig. 5c–m, 8b, 9b). Such features can be interpreted as implying short sediment transport from an adjacent and voluminous magmatic source typical of a rapidly eroding active magmatic arc and are considered as characteristic of sedimentation in an active-margin tectonic setting. Indeed, majority of zircons from these samples have high Th/U ratios (Supplementary material B), typical magmatic internal zoning and well-preserved crystal shapes again supporting short transport directly from the adjacent plutonic source (Fig. 4c–i). The presence of amphibole in some of the drill-cores suggests at least partly volcano-sedimentary nature and synvolcanic sedimentation. The overall lithological variability of drill-cores (Dudek et al., 1980) is compatible with relatively immature turbiditic deposition. Altogether, the Ediacaran sequences were likely deposited in shallow proximal parts of the Cadomian synorogenic (fore- or back-arc) basin dominantly sourced by the adjacent magmatic arc.

In contrast, sample UD 11 from the Moravo–Silesian Zone contains both a significant Neoproterozoic age peak and large amount of Mesoproterozoic and Neoarchean zircons (Fig. 5j) similar to the studied Tonian samples. On the other hand, sample UD 20 from the Micaschist Zone has the dominant youngest Neoproterozoic age peak and significant age group around c. 2.0 Ga (Fig. 5m) indicating both proximity of the Cadomian magmatic arc and the Paleoprotorezoic basement.

5.2. ***Possible sources for individual zircon age populations***

Possible sources for individual age groups of the studied samples can be traced from youngest to oldest as follows. Except for the Tonian sequences, the youngest Cryogenian–Ediacaran population forms the major age peak in the majority of the studied samples (Fig. 9a, 10b–d). This age group at c. 650–560 Ma fits well with the main interval of magmatic activity of the Brno Massif (Hanžl et al., 2019; Soejono et al., 2017; Timmerman et al., 2019), as well as the spread of protolith ages of the Moravo–Silesian orthogneisses (Friedl et al., 2000; Kröner et al., 2000; Mazur et al., 2010; Soejono et al., 2017). Therefore, these most abundant zircons could be interpreted as a juvenile detritus coming directly from the neighbouring magmatic arc system, consistent with an inferred active margin depositional setting. The large spread of $\varepsilon_{Hf(t)}$ values (–24 to +13) of the Neoproterozoic zircons from the Ediacaran sequences, with model ages between 2.7 and 0.75 Ga, suggests mixing of juvenile mantle-derived magmas with mature crustal material, typical of large continental magmatic arc systems. Similarly, a wide range of $\varepsilon_{Hf(t)}$ values (–27 to +14) with model ages between 2.8 and 0.73 Ga of the Neoproterozoic zircons from the Micaschist Zone can be interpreted as reflecting a combination of juvenile magmas and reworking of the Paleo-and Mesoproterozoic crust.

The provenance of older zircons is less obvious and their ages need to be related to the most probable source regions. The c. 1.0 Ga age peak in the Tonian sequences and the Moravo–Silesian Zone samples corresponds to the Grenville-age sources related to the formation of the Rodinia supercontinent (Dalziel, 1997; Hoffman, 1991; Li et al., 2008). The wide range of Mesoproterozoic ages forms two peaks at c. 1.2 and 1.5 Ga (Fig. 5, 9a, c). In the possible source regions, the c. 1.7–1.0 Ga magmatic complexes are known from the Sveconfennian and Sveconorwegian basement of the southwestern Baltica (Fig. 9c; Bingen at al., 2011; Bogdanova et al., 2008) but also from the Sunsás, Rondonian-San Ignácio and Rio Negro-Juruena belts of the Amazonian Craton (Fig. 9d; Cordani and Teixeira, 2007; Tassinari and Macambria, 1999; Teixeira, 1989). Similarly, the Paleoproterozoic and Neoarchean zircon population at c. 3.0–1.8 Ga could have been derived either from the Svecofennian, Fennoscandian and Ukrainian Shield sources of Baltica (Fig. 9c; Bogdanova et al., 2008; Kuznetsov et al., 2010) or Ventauri-Tapajós, Maroni-Itacaiúnas and Central Amazonian belts of the Amazonia (Fig. 9d; e.g. Tassinari and Macambria, 1999). The slightly negative to positive $\varepsilon_{Hf(t)}$ values and model ages between 2.4 and 1.3 Ga of the Paleo-and Mesoproterozoic zircons imply a juvenile nature of magma sources, with minor recycling of Paleoproterozoic crust indicated only by a small number of zircons with subchondritic $\varepsilon_{Hf(t)}$ values. Unfortunately, no Paleoproterozoic zircons from the Edicaran sequences were analysed for Hf isotopic composition due to the small grain sizes.

The Ediacaran sequences and the Micaschist Zone show remarkable lack of Mesoproterozoic ages between c. 1.6–1.0 Ga (Fig. 5c–i, k) that indicates no or very rare magmatic activity in the source area at the time. Apart from dominant Neoproterozoic zircons, they also contain minor but important Paleoproterozoic age peak (Fig. 5c–i, 9b). Such a pattern has been generally interpreted as provenance a signature of the Eburnean basement of the West African Craton and Sahara Metacraton (e.g. Ennih and Liégeois, 2008; Fernández-Suaréz et al., 2002; Linnemann et al., 2004; Meinhold et al., 2013; Samson et al., 2005).

In summary, the above-described correlations show that both the Baltica and Amazonia cratons could provide clastic material for the pre-Cadomian successions (Fig. 9). Thus, the detrital age data do not allow us to discriminate between a Baltica-adjacent or Amazonia-adjacent position of the Brunovistulian Domain during the Tonian. In contrast, the Brunovistulian Ediacaran basin was sourced almost exclusively from the late Neoproterozoic active magmatic arc.

*5.3. **Correlation with other parts of the Bohemian Massif***

The individual parts of the Brunovistulian Domain could be compared with the surrounding units of the Bohemian Massif based on the detrital zircon age similarities. A scarcity of Mesoproterozoic zircon ages (c. 1.7–1.0 Ga) in metasediments of the rest of the Bohemian Massif is broadly considered as a fundamental difference from the Brunovistulian Domain and as a major argument for their different provenance (e.g. Friedl et al., 2000; Linnemann et al., 2004). The new presented data confirmed significant record of Mesoproterozoic ages in the Tonian host-rocks of the Brno Massif and the Moravo–Silesian Zone (Fig. 10a, c). These age spectra show remarkable similarity to the Mesoproterozoic metasediments of the Drosendorf Unit of the Moldanubian Zone in Austria (Fig. 10e; Lindner et al., 2020; Sorger et al., 2020). The Moldanubian Dobra orthogneiss of the Drosendorf Unit sequence thus can be compared to the Moravo–Silesian orthogneiss bodies such as the Bíteš gneiss (Friedl et al., 2004) and metasedimentary packages implying their close affinity, which was suspected by some authors based on lithological similarities (e.g. Frasl, 1968, 1970; Matura, 2003). Moreover, the presence of rare fragments of the c. 2.0 Ga Paleoproterozoic basement in both the Brunovistulian Domain (Collett et al., 2021; Żelażniewicz and Fanning, 2020) and Moldanubian Zone (Trubač et al., 2012; Wendt et al., 1993) indicated that both these domains share a common crust.

However, the rest of the studied samples from the Ediacaran sequences are uniformly dominated by the Neoproterozoic ages at c. 600 Ma and show also a subordinate but significant Paleoproterozoic age group in the interval of c. 2.0–1.8 Ga (Fig. 10b). Surprisingly, the detrital zircon age populations show a distinct low abundance of the Mesoproterozoic ages in all the seven samples from the Ediacaran sequences (Fig. 10b). Comparison with the published data shows that this age pattern is indistinguishable from those from the Micaschist Zone, Moldanubian Zone and Teplá–Barrandian Unit (Fig. 10d, f, g; for references see caption of Fig. 8). The cumulative age distributions of these units follow the same concave trend dominated by the Neoproterozoic ages as the Ediacaran successions (Fig. 8b) indicating analogous deposition in the basins adjacent to the active Cadomian magmatic arc. This result is compatible with the model of the Neoproterozoic–earliest Cambrian (meta-) sedimentary successions of the Teplá–Barrandian Unit and Moldanubian Zone both interpreted as a Cadomian accretionary wedge dominated by the arc-derived detritus (Drost et al., 2011; Hajná et al., 2017, 2018; Soejono et al., 2020).

Combined age data from the Micaschist Zone (Fig. 10d) are essentially identical to those from the Moldanubian Zone (Fig. 10f). This resemblance supports the idea that the Micaschist Zone represents strongly deformed and retrogressed Moldanubian margin, as proposed already by Suess (1912) and Fuchs (1976). Moreover, similar zircon Hf isotopic signatures of the Ediacaran sequences and the Micaschist Zone imply identical age and nature of the magma sources and possible Paleogeographic neighbourhood of the Brunovistulian Domain and the Moldanubian Zone during the Neoproterozoic.

5.4. Do the Mesoproterozoic zircons represent real paleogeographic fingerprint?

These close similarities discussed above cast some doubts on the model of the Brunovistulian Domain and other parts of the Bohemian Massif as mutually independent crustal blocks in pre-Varican times. The presence of the Mesoproterozoic zircons as a critical feature of the detrital and xenocrystic zircon age patterns of the Brunovistulian Domain in contrast to the rest of the Bohemian Massif (Friedl et al., 2000; Linnemann et al., 2004; Mazur et al., 2012) is not as unequivocal as previously suggested.

In order to explain this new contradiction, other factors such as the availability of the Mesoproterozoic sources and spatial variability of sedimentary processes should be taken into account. The scarcity of the Mesoproterozoic ages in many Brunovistulian samples indicates that such old sources were not exposed or rare in the source region during the Neoproterozoic deposition time. Mesoproterozoic zircon-rich Tonian basement is even in the present-day erosional level exposed only very rarely as roof pendants (up to 1000 m large) in the granodiorites of the Brno Massif. While the Tonian basement is not a major source for the Ediacaran sediments, their detrital signature can be observed in inherited zircons included in Neoproterozoic granitoids. Nonetheless, Mesoproterozoic xenocrysts while abundant in the Neoproterozoic orthogneisses of the Moravo–Silesian Zone and adjacent areas (Friedl et al., 2004; Lindner et al., 2020; Mazur et al., 2010; Oberc-Dziedzic et al., 2003) are scarce in the granodiorites of the easterly Brno Massif (Hanžl et al., 2019; Timmerman et al., 2019; Soejono et al., 2017; Svojtka et al., 2017). This difference can be simply explained by the overall abundance of zircons in the metasedimentary magma source of the S-type granites and their general scarcity in the I-type magmas (see also discussion in Soejono et al., 2017).

An obvious lack of the Mesoproterozoic ages in the Ediacaran sequences as well as in the Moldanubian Zone and Teplá–Barrandian Unit (Fig. 8b, 9) point to a similar source of detritus for all these units and suggests the possibility that they belonged to a continuous crustal domain. The lack of Mesoproterozoic ages could be explained by the overwhelming dominance of the Neoproterozoic detritus originating from the Cadomian magmatic arc directly adjacent to the sedimentary basin. Such detrital zircon age populations potentially do not record the real age pattern of deep continental basement but exclusively the source actually exposed at the time of deposition such as a large stratovolcanos of the active volcanic arc. The cases that the part of detrital population can be shaded by the dominant and nearest source or it may become unavailable due to previous erosion have been recently documented in many studies (e.g. Andersen et al., 2016; Ghienne et al., 2018; Jackson et al., 2019; Konopásek et al., 2017; Percival et al., 2021; Saylor et al., 2013).

*5.5. **Did the Rheic suture exist between the Brunovistulian Domain and the Moldanubian Zone?***

The existence of a Rheic oceanic suture (e.g. Nance et al., 2010) at the eastern margin of the Bohemian Massif and continuation of the Rhenohercynian Zone from northwest Europe to the Brunovistulian Domain is critical for understanding of not only the pre-collisional but also the Variscan evolution. Moores (1981) defined a set of criteria for recognition of suture zones in orogenic belts, including the presence of ophiolites, paired metamorphic belts and magmatic arcs, involvement of the continental margin sequences, contrasting geochronological provinces and structural, paleomagnetic and stratigraphic differences across the suture. Of these criteria, the presence of ophiolites (Finger et al., 1998; Finger and Steyer, 1995; Höck et al., 1997) and eclogites (Collett et al., 2021; Konopásek et al., 2002; Štípská et al., 2006) at the Late Devonian–early Carboniferous boundary between the Moravo–Silesian Zone and Moldanubicum were considered as arguments for the existence of the Rheic suture zone (e.g. Jastrzębski et al., 2013). However, early Cambrian protolith age of eclogite sample from this tectonic boundary and intra-continental rift signatures of hanging-wall Letovice and Staré Město complexes indicate that the presence of a large Ordovician Rheic oceanic basin between the Moldanubian and Brunovistulian domains is not likely (Collet et al., 2021; Soejono et al., 2010). On the contrary, the main east-dipping Early Devonian subduction system located at the opposite (western) side of the Bohemian Massif is supported by the presence of 400–390 Ma old HP rocks decorating the main NE–SW trending Variscan suture (e.g. Collett et al., 2018; Tabaud et al., 2021), parallel to a Middle–Late Devonian magmatic arc located east of the suture zone (e.g. Deiller et al., 2021; Žák et al., 2011), as well as by geophysical data (Franěk et al., 2011; Guy et al., 2011). The subduction system of the eastern margin of the Bohemian Massif is most likely responsible for a closure of a large Paleozoic back-arc system as proposed by Schulmann et al. (2009; 2014b) and modelled by Dymkova et al. (2016). Our study further coins this idea as the Neoproterozoic sequences of both the Brunovistulian Domain and central part of the Bohemian Massif share very similar clastic zircon age and Hf isotopic patterns. This is another independent argument excluding the existence of a large Cambro–Ordovician oceanic domain between them. However, an unconstrained gap of c. 200 My remains between the Ediacaran and Late Devonian configurations discussed above, and the hypothetical opening and subsequent closure of a large oceanic domain between here cannot be completely ruled out.

5.6. ***Implications for pre-Variscan evolution of the Bohemian Massif***

5.6.1. Neoproterozoic paleogeographic position

When discussing the paleogeography of the Brunovistulian Domain, it is necessary to consider the Neoarchean and Paleoproterozoic age of the basement (Collett et al., 2021; Żelaźniewicz and Fanning, 2020), as well as the inferred Tonian (c. 930 Ma) maximum depositional ages (Fig. 6a, b) and tectonic setting (Fig. 8a) of the pre-Cadomian sequences. Moreover, both Archean and especially Mesoproterozoic detritus sources had to be available at the time of deposition. The calculated maximum depositional ages correspond exactly to the final stage of the Grenville orogeny and Rodinia continental assembly (e.g. Ernst et al., 2008; Li et al., 2008; Scotese, 2009). If these calculated maximum depositional ages approximate the samples true depositional ages, then an interior Rodinia position (star 1 in Fig 11a) is possible. In this scenario, the sediments could have been deposited in a syncollisional basin at the southeastern Baltica–northern Amazonia junction (Fig. 11a, b). Mesoproterozoic detritus could have been sourced from the Grenville-age collisional belt, while both Archean and Paleoproterozoic basement are well represented in both the Amazonia and Baltica cratons.

On the other hand, these sequences could have been deposited significantly later as discussed above. In that case, they might record late Tonian intracontinental extension (Fig. 11b) related to the Rodinia break-up (at c. 800–700 Ma; e.g. Ernst et al., 2008; Li et al., 2008; Scotese, 2009). Furthermore, a location on the passive margin developed along the Rodinia periphery (Fig. 11c) is also permissible (e.g. Bogdanova et al., 2008). Two possible Rodinia periphery positions on the southern to south-eastern margin of Baltica (star 2) and on the eastern margin of Amazonia (star 3) are shown in Fig. 11. Such external positions are in accord with the subduction-related nature of the late Tonian (c. 730 Ma) Metabasite Zone

(Hanžl et al., 2019). However, these passive margin alternatives would require long-distance transport of clastic material in order to provide the Mesoproterozoic detritus (Fig. 11a). Moreover, studies of modern drainage systems (e.g. Blum et al., 2018; Singh et al., 2007) show that sedimentary transport over continental distances may be possible. For example, the Mesoproterozoic zircons have been reported from Neoproterozoic sequences along the eastern Baltica margin (e.g. Kuznetsov et al., 2014) although no such old basement is known there (Bogdanova et al., 2008).

It is generally accepted that the Brunovistulian Domain was involved in the Ediacaran magmatic arc system (Finger et al., 2000a; Hanžl et al., 2019; Soejono et al., 2017). Such a Pacific-type subduction system operated during the Cadomian orogeny (at c. 650–570 Ma) along the entire northern Gondwana margin (e.g. Murphy et al., 2004; Nance et al., 1991) and the Timanian orogeny (at c. 610–560 Ma) occurred in northeastern Baltica (e.g. Gee and Pease, 2004; Kuznetsov et al., 2010). The above-mentioned options for the Tonian paleogeography imply several possible positions of the Brunovistulian Domain after the final break-up of Rodinia at c. 700 Ma (Ernst et al., 2008; Li et al., 2008; Scotese, 2009). In the case of the interior Rodinia position (star 1 in Fig. 11a), it could have remained attached to the newly separated northern Amazonia margin (star 1 in Fig. 11d), while the opposing Baltica side can likely be excluded due to the existence of a passive margin at that time (Krzywiec et al., 2018; Mazur et al., 2018; Poprawa, 2019; Żelaźniewicz et al., 2020). However, late Ediacaran rifting of Baltica, presumably from Amazonia, has been suggested by U–Pb zircon dating (c. 590–550 Ma) of the Volyn volcanic province in the southeastern Baltica (e.g. Poprawa et al., 2020; Shumlyansky et al., 2016). In this case, a long-lasting magmatic arc system could not have developed there during the Ediacaran. Considering the alternative Rodinia exterior positions (stars 2 and 3 in Fig. 11a), this would place the Brunovistulian

Domain close to either southeastern Baltica or eastern Amazonia (stars 2 and 3 in Fig. 11d). Traditional models (e.g. Murphy et al., 2004; Nance and Murphy, 1994; Nance et al., 1991) for the Cadomian-Avalonian arc complexes assume their distribution on the crustal blocks separated from the margins of the Amazonian or West African cratons, while Ediacaran arc-related magmatism is not yet known from the southeastern to southwestern margins of Baltica. This rather favors an Amazonian provenance for the Brunovistulian Domain. On the other hand, the paleontological (Vavrdová et al., 2003) and newest paleomagnetic data suggest that the Brunovistulian Domain was part of peri-Baltica already in the Ediacaran (Nawrocki et al., 2021), and recent zircon provenance studies from southern Baltica (e.g. Francovschi et al., 2021; Paszkowski et al., 2021) have indicated detrital input from an as yet unknown convergent margin during the latest Ediacaran and early Cambrian. The Brunovistulian Domain could have belonged to the hypothetical southern Baltica active margin as a potential continuation of the northeastern Timanides. Theoretically, it could have been dextrally shifted along the Trans-European Suture Zone (e.g. Pharaoh, 1999) during the Paleozoic to the current position in the Variscan belt. Large-scale dextral movements have been interpreted as resulted from the overall clockwise rotation of Gondwana in respect to Baltica (e.g. Edel et al., 2018; Oriolo et al., 2021). Nevertheless, the above mentioned paleogeographical clues are often contradictory, and thus, the Neoproterozoic Brunovistulian configuration and its path to the present position still remain controversial.

5.6.2. Model of the Neoproterozoic configuration of the Bohemian Massif

Strong geochronological similarities of the westerly parts of the Bohemian Massif with the Ediacaran metasedimentary complexes building a large part of the Brunovistulian Domain suggest that all these units belonged to a single Neoproterozoic crustal domain and probably were never separated by a significant ocean. The Brunovistulian/Moldanubian boundary thus in our view represents a Variscan deformation zone (orogenic hinterland–foreland transition) rather than a true terrane suture. Such an interpretation obviously implies that the Rheic suture does not continue from northwestern Europe into the Bohemian Massif.

Our correlation shows that the Neoproterozoic basins on both sides of an active magmatic arc belt were identically filled mostly by arc-related detritus. The Teplá–Barrandian Unit is broadly considered as a Cadomian accretionary wedge (Drost et al., 2011; Hajná et al., 2017, 2018), with the Jílové Belt as an associated Neoproterozoic magmatic arc. However, the small-scale volcanic succession of the Jílové Belt can be interpreted merely as a shallow part of an intra-oceanic volcanic arc (Sláma et al., 2008a; Waldhausrová, 1984). The giant and long-lasting subduction would require the existence of a significantly larger and long lasting continental magmatic arc system as it is recently known from the Eastern Pacific. We propose that the belt of Neoproterozoic magmatic arc complexes of the Brunovistulian Domain (e.g. Brno Massif) represents the suitable candidate. Therefore, the studied Ediacaran sequences can be interpreted as being deposited in a back-arc basin behind the active Cadomian magmatic arc, while the Teplá–Barrandian Unit and oldest parts of the Moldanubian Zone were located in an accretionary wedge position on the opposite side (Fig. 11 e).

The presented idea of the central and eastern parts of the Bohemian Massif viewed as a single Neoproterozoic crustal segment offers a new pre-collisional evolutionary model alternative to the prevailing hypothesis of the Rheic suture and contrasting primary paleogeographic positions of individual domains. Moreover, the presented paleogeographic discussions may imply a greater role of peri-Baltican material within the Variscan belt, potentially significantly altering our understanding of European Paleozoic geology in general.

6. Conclusions

The presented detrital zircon geochronological and Hf isotopic data from metasedimentary sequences of the Brunovistulian Domain combined with published studies allow to draw the following conclusions:

1) Studied metasedimentary complexes of the Brunovistulian Domain show contrasting detrital zircon ages and Hf isotopic patterns.
2) The Tonian sequences were deposited in a basin either in the interior or on the periphery of Rodinia, and their clastic material was derived dominantly from the Paleo- and Mesoproterozoic basement of Baltica and/or Amazonia.
3) The Ediacaran sequences were deposited in a back-arc basin and sourced almost exclusively from an active continental magmatic arc.
4) Age population of the Ediacaran sequences records almost exclusively a dominant adjacent magmatic arc source and does not represent the full age pattern of the continental basement.
5) The change in detrital zircon U–Pb age and Hf record of the Brunovistulian Domain that took place between the early and late Neoproteorozoic probably reflects the Neoproterozoic plate-tectonic reconfiguration from the Rodinia formation/break-up to the evolution of the Gondwana or Baltica active margin.
6) Correlation of detrital zircon age populations from different parts of the Bohemian Massif revealed similarities challenging the main arguments for an existence of the Rheic suture between the Brunovistulian Domain and the Moldanubian Zone and suggests an alternative pre-collisional model of the Bohemian Massif as a single Neoproterozoic crustal domain.

Acknowledgements

This study was funded by Research Project no. 310960 (Strategic Research Plan of the Czech Geological Survey-DKRVO/ČGS 2018–2022). J. Sláma was supported by the Czech Academy of Science institutional support to the Institute of Geology of the Czech Academy of Science (RVO 67985831). We thank F. Veselovský for mineral separation, N. Novotná for CL images and Hf analyses and A. Dudek for providing of drill-cores. We would also like to thank Stanislaw Mazur and an anonymous reviewer for their constructive comments and Wilson Teixeira for editorial handling.

Online Supplementary material

Supplementary Material A – Micro- and macro-photographs of the studied samples

Supplementary Material B – U–Pb and Hf isotopic data

References:

Andersen, T., Kristoffersen, M., Elburg, M.A., 2016. How far can we trust provenance and crustal evolution information from detrital zircons? A South African case study. Gondwana Res. 34, 129–148. doi:10.1016/j.gr.2016.03.003

Andersen, T., Kristoffersen, M., Elburg, M.A., 2017. Visualizing, interpreting and comparing detrital zircon age and Hf isotope data in basin analysis – a graphical approach. Basin Res. 38, 42–49. doi.org/10.1111/bre.12245

Belka, Z., Valverde-Vaquero, P. ,Dörr, W., Ahrendt, H., Wemmer, K., Franke W., Schäfer J., 2002. Accretion of first Gondwana-derived terranes at the margin of Baltica. Geol. Soc. Spec. Publ. 201, 19–36. doi.org/10.1144/GSL.SP.2002.201.01.02

Belousova, E.A., Kostitsyn, Y.A., Griffin, W.L., Begg, G.C., O'Reilly, S.Y., Pearson, N.J., 2010. The growth of the continental crust: constraints from zircon Hf-isotope data. Lithos, 119, 457–466. doi:10.1016/j.lithos.2010.07.024

Bindeman, I.N., Melnik, O.E., 2016. Zircon survival, rebirth and recycling during crustal melting, magma crystallization, and mixing based on numerical modelling. Journal of Petrology, 57, 437–460. doi:10.1093/petrology/egw013

Bingen, B., Belousova, E. A., Griffin, W.L., 2011. Neoproterozoic recycling of the Sveconorwegian orogenic belt: Detrital-zircon data from the sparagmite basins in the Scandinavian Caledonides. Precambrian Res. 189, 347–367. doi:10.1016/j.precamres.2011.07.005

Blichert-Toft, J.E., Albaréde, F., 1997. The Lu–Hf isotope geochemistry of chondrites and the evolution of the mantle-crust system. Earth. Planet. Sci. Lett. 148, 243–258. doi: 10.1016/S0012-821X(97)00040-X

Blum, M., Rogers, K., Gleason, J., Najman, Y., Cruz, J., Fox, L., 2018. Allogenic and Autogenic Signals in the Stratigraphic Record of the Deep-Sea Bengal Fan. Sci. Rep. 8, 1–13. doi:10.1038/s41598-018-25819-5

Bogdanova, S.V, Bingen, B., Gorbatschev, R., Kheraskova, T.N., Kozlov, V.I., Puchkov, V.N., Volozh, Y.A., 2008. The East European Craton (Baltica) before and during the assembly of Rodinia. Prcambrian Res. 160, 23–45. doi:10.1016/j.precamres.2007.04.024

Bukovská, Z., Soejono, I., Vondrovic, L., Vavro, M., Souček, K., Buriánek, D., Dobeš, P., Švagera, O., Waclawik, P., Řihošek, J., Verner, K., Sláma, J., Vavro, L., Koníček, P., Staš, L., Pécskay, Z., Veselovský, F., 2019. Characterization and 3D visualization of underground research facility for deep geological repository experiments: A case study of underground research facility Bukov, Czech Republic. Eng. Geol. 105186. doi:https://doi.org/10.1016/j.enggeo.2019.105186

Buła, Z., Habryn, R., Jachowicz-Zdanowska, M., Żaba, J., 2015. The precambrian and lower paleozoic of the brunovistulicum (eastern part of the upper silesian block, southern Poland) – The state of the art. Geol. Q. 59, 123–134. doi:10.7306/gq.1203

Buła, Z., Jachowicz, M., 1996. The Lower Paleozoic sediments in the Upper Silesian Block. Geol. Q. 40, 299–336.

Cawood, P.A., Hawkesworth, C.J., Dhuime, B., 2012. Detrital zircon record and tectonic setting. Geology, 40, 875–878. doi:10.1130/G32945.1

Cawood, P.A., Strachan, R.A., Pisarevsky, S.A., Gladkochub, D.P., Murphy, J.B., 2016. Linking collisional and accretionary orogens during Rodinia assembly and breakup: Implications for models of supercontinent cycles. Earth Planet. Sci. Lett. 449, 118–126. doi:10.1016/j.epsl.2016.05.049

Chauvel, C., Blichert-Toft, J., 2001. A hafnium isotope and trace element perspective on melting of the depleted mantle. Earth Planet. Sci. Lett. 190, 137–151. doi10.1016/S0012-821X(01)00379-X

Chlupáč, I., 1989. Fossil communities in the metamorphic Lower Devonian of the Hrubý Jeseník Mts., Czechoslovakia. Neues Jahrb. fur Geol. Palaontol. Abh. 177, 367–392.

Chu, N.C., Taylor, R.N., Chavagnac, V., Nesbitt, R.W., Boella, R.M., Milton, J.A., German, C.R., Bayon, G., Burton, K., 2002. Hf isotope ratio analysis using multi-collector inductively coupled plasma mass spectrometry: an evaluation of isobaric interference corrections. J. Anal. Atom. Spectrom. 17, 1567–1574. doi:10.1039/b206707b

Cardona, A., Cordani, U.G., Ruiz, J., Valencia, V.A., Armstrong, R., Chew, D., Nutman, A., Sanchez, A.W., 2009. U–Pb zircon geochronology and Nd isotopic signatures of the Pre-Mesozoic metamorphic basement of the Eastern Peruvian Andes: growth and provenance of a Late Neoproterozoic to Carboniferous accretionary orogen on the northwest margin of Gondwana. J. Geol. 117, 285–305.

Collett, S., Schulmann, K., Štípská, P., Míková, J., 2020. Chronological and geochemical constraints on the pre-variscan tectonic history of the Erzgebirge, Saxothuringian Zone. Gondwana Res. 79, 27–48. doi:10.1016/j.gr.2019.09.009

Collett, S., Štípská, P., Schulmann, K., Peřestý, V., Soldner, J., Anczkiewicz, R., Lexa, O., Kylander-Clark, A., 2018. Combined Lu-Hf and Sm-Nd geochronology of the Mariánské Lázně Complex: New constraints on the timing of eclogite- and granulite-facies metamorphism. Lithos, 304–307, 74–94. doi:10.1016/j.lithos.2018.02.007

Collett, S., Štípská, P., Schulmann, K., Míková, J., Kröner, A., 2021. Tectonic significance of the Variscan suture between Brunovistulia and the Bohemian Massif. J. Geol. Soc. London. 178, doi:10.1144/jgs2020-176

Cordani, U.G., Teixeira, W., 2007. Proterozoic accretionary belts in the Amazonian Craton. In: Hatcher Jr., R.D., Carlson, M.P., McBride, J.H., Martínez-Catalán, J.R. (Eds.), 4-D Framework of Continental Crust: Geological Society of America, Memoirs 200, 297–320.

Dalziel, I.W.D., 1997. Neoproterozoic-paleozoic geography and tectonics: Review, hypothesis, environmental speculation. Bull. Geol. Soc. Am. 109, 16–42. doi:10.1130/0016-7606(1997)109<0016:ONPGAT>2.3.CO;2

Deiller, P., Štípská, P., Ulrich, M., Schulmann, K., Collett, S., Peřestý, V., Hacker, B., Kylander-Clark, A., Whitechurch, H., Lexa, O., Pelt, E., Míková, J., 2021. Eclogite subduction wedge intruded by arc-type magma: The earliest record of Variscan arc in the Bohemian Massif. Gondwana Res. 99, 220–246. doi:10.1016/j.gr.2021.07.005

Dickinson, W.R., Gehrels, G.E., 2009. Use of U–Pb ages of detrital zircons to infer maximum depositional ages of strata: A test against a Colorado Plateau Mesozoic database. Earth Planet. Sci. Lett. 288, 115–125. doi:10.1016/j.epsl.2009.09.013

Drost, K., Gerdes, A., Jeffries, T., Linnemann, U., Storey, C., 2011. Provenance of Neoproterozoic and early Paleozoic siliciclastic rocks of the Teplá-Barrandian unit (Bohemian Massif): Evidence from U–Pb detrital zircon ages. Gondwana Res. 19, 213–231. doi:10.1016/j.gr.2010.05.003

Dudek, A., 1980. The crystalline basement block of the Outer Carpathians in Moravia, BrunoVistulicum. Rozpr. Čs. Akad. Věd., 3–85.

Dymkova, D., Gerya, T., Burg, J.P., 2016. 2D thermomechanical modelling of continent-arc-continent collision. Gondwana Res. 32, 138–150. doi:10.1016/j.gr.2015.02.012

Edel, J.B., Schulmann, K., Lexa, O., Lardeaux, J.M., 2018. Late Palaeozoic palaeomagnetic and tectonic constraints for amalgamation of Pangea supercontinent in the European

Variscan belt. Earth-Science Rev. 177, 589–612. doi:10.1016/j.earscirev.2017.12.007

Ernst, R.E., Wingate, M.T.D., Buchan, K.L., Li, Z.X., 2008. Global record of 1600-700 Ma Large Igneous Provinces (LIPs): Implications for the reconstruction of the proposed Nuna (Columbia) and Rodinia supercontinents. Precambrian Res. 160, 159–178. doi:10.1016/j.precamres.2007.04.019

Ennih, N., Liégeois, J.-P., 2008. The boundaries of the West African craton, with special reference to the basement of the Moroccan metacratonic Anti-Atlas belt. Geol. Soc. Spec. Publ. 297, 1–17. Doi: 10.1144/SP297.1

Fedo, C.M., Sircombe, K.N., Rainbird, R.H., 2003. Detrital zircon analysis of the sedimentary record. In: Hanchar, J.M., Hoskin, P.W. (Eds.), Zircon. Rev. Min. Geochem. 53, 277–304. doi: 10.2113/0530277

Fernández-Suárez, J., Gutiérrez Alonso, G., Jeffries, T.E., 2002. The importance of along margin terrane transport in northern Gondwana: insights from detrital zircon parentage in Neoproterozoic rocks from Iberia and Brittany. Earth Planet. Sci. Lett. 204, 75–88. doi: 10.1016/S0012-821X(02)00963-9

Finger, F., Hanžl, P., Pin, C., von Quadt, A., Steyrer, H.P., 2000a. The Brunovistulian, Avalonian Precambrian sequence at the eastern end of the Central European Variscides? In, Franke, W., Haak, V., Oncken, O., Tanner, D. (Eds.), Orogenic Processes, Quantification and Modelling in the Variscan Belt. Geol. Soc. Spec. Publ. 179, 103–112. doi: 10.1144/GSL.SP.2000.179.01.08

Finger, F., Frasl, G., Dudek, A., Jelínek, E., Thöni, M., 1995. Igneous activity (Cadomian plutonism in the Moravo-Silesian basement). In: Dallmeyer RD, Franke W, Weber K (eds) Pre-Permian Geology of Central and Eastern Europe. Springer, Berlin, 495–507.

Finger, F., Schitter, F., Riegler, G., Krenn, E., 1999. The history of the Brunovistulicum: total-Pb monazite ages from the metamorphic complex. Geolines, 8, 22–23.

Finger, F., Steyrer, H. P., 1995. A tectonic model for the eastern Variscides: Indications from a chemical study of amphibolites in the south–eastern Bohemian Massif. Geol. Carpath. 46. 3. 137–150.

Finger, F., Tichomirowa, M., Pin, C., Hanžl, P., 2000b. Relics of early-Panafrican metabasite–metarhyolite formation in the Brno Massif, Moravia, Czech Republic. Int Journ Earth Sciences, 89, 328–335. Doi: 10.1007/s005310000084

Finger, F., von Quadt, A., Pin, C., Steyrer, H.P., 1998. The ophiolite chain along the western Moravo-Silesian plate margin–a trace of the Rheic suture? Act. Univ. Carol., Geol. 42, 244–245.

Francovschi, I., Grădinaru, E., Li, H., Shumlyanskyy, L., Ciobotaru, V., 2021. U–Pb geochronology and Hf isotope systematics of detrital zircon from the late Ediacaran Kalyus Beds (East European Platform): palaeogeographic evolution of southwestern Baltica and constraints on the Ediacaran biota. Precambrian Res. 355, 106062. doi:10.1016/j.precamres.2020.106062

Franěk, J., Schulmann, K., Lexa, O., Tomek, C., Edel, J.B., 2011. Model of syn-convergent extrusion of orogenic lower crust in the core of the Variscan belt: Implications for exhumation of high-pressure rocks in large hot orogens. J. Metamorph. Geol. 29, 53–78. doi:10.1111/j.1525-1314.2010.00903.x

Franke, W., 2000. The mid-European segment of the Variscides: tectonostratigraphic units, terrane boundaries and plate tectonic evolution. Geol. Soc. Spec. Publ. 179, 35–61. doi: 10.1144/GSL.SP.2000.179.01.05

Frasl, G., 1968. The Bohemian Massif in Austria, Moravian Zone. - Guide to Excursion 32c, International Geology Congress, XXIII. Session, 13–24, Prague.

Frasl, G., 1970. Zur Metamorphose und Abgrenzung der Moravischen Zone im niederösterreichischen Waldviertel. Nachr. Dtsch. Geol. Gesell. 2, 55–60, Hannover.

Friedl, G., Finger, F., McNaughton, N.J., Fletcher, I.R., 2000. Deducing the ancestry of terranes, SHRIMP evidence for South America-derived Gondwana fragments in central Europe. Geology, 28, 1035–1038. doi: 10.1130/0091-7613(2000)28<1035:DTAOTS>2.0.CO;2

Friedl, G., Finger, F., Paquette, J.L., von Quadt, A., McNaughton, N.J., Fletcher, I.R., 2004. Pre-Variscan geological events in the Austrian part of the Bohemian Massif deduced from U/Pb zircon ages. Int. J. Earth Sci. 93, 802–823. doi: 10.1007/s00531-004-0420-9

Fritz, H., Dallmeyer, R. D., Neubauer, F., 1996. Thick-skinned versus thin-skinned thrusting: Rheology controlled thrust propagation in the Variscan collisional belt (The southeastern Bohemian Massif, Czech Republic-Austria). Tectonics, 15, 1389–1413. doi: 10.1029/96TC01098

Gee, D.G., Pease, V., 2004. The Neoproterozoic Timanide Orogen of eastern Baltica: introduction. Geol. Soc. London, Mem. 30, 255. doi: 10.1144/GSL.MEM.2004.030.01.01

Gee, D.G., Ladenberger, A., Dahlqvist, P., Majka, J., Be'Eri-Shlevin, Y., Frei, D., Thomsen, T., 2014. The baltoscandian margin detrital zircon signatures of the central scandes. Geol. Soc. Spec. Publ. 390, 131–155. doi:10.1144/SP390.20

Gehrels, G., 2014. Detrital zircon U–Pb geochronology applied to tectonics. Annu. Rev. Earth Planet. Sci. 42, 127–149. doi: 10.1146/annurev-earth-050212-124012

Ghienne, J.F., Benvenuti, A., El Houicha, M., Girard, F., Kali, E., Khoukhi, Y., Langbour, C., Magna, T., Míková, J., Moscariello, A., Schulmann, K., 2018. The impact of the end-Ordovician glaciation on sediment routing systems: A case study from the Meseta (northern Morocco). Gondwana Res. 63, 169–178. doi:10.1016/j.gr.2018.07.001

Guy, A., Edel, J.B., Schulmann, K., Tomek, C., Lexa, O., 2011. A geophysical model of the Variscan orogenic root (Bohemian Massif): Implications for modern collisional orogens. Lithos, 124, 144–157. doi:10.1016/j.lithos.2010.08.008

Habryn, R., Krzeminska, E., Krzeminski, L., 2020. Detrital zircon age data from the conglomerates in the Upper Silesian and Małopolska Blocks and their implications for the pre-Variscan tectonic evolution (S Poland). Geol. Q. 64, 321–341. doi:10.7306/gq1539

Hajná, J., Žák, J., Dörr, W., 2017. Time scales and mechanisms of growth of active margins of Gondwana: A model based on detrital zircon ages from the Neoproterozoic to Cambrian Blovice accretionary complex, Bohemian Massif. Gondwana Res. 42, 63–83. doi:10.1016/j.gr.2016.10.004

Hajná, J., Žák, J., Dörr, W., Kachlík, V., Sláma, J., 2018. New constraints from detrital zircon ages on prolonged, multiphase transition from the Cadomian accretionary orogen to a passive margin of Gondwana. Precambrian Res. 317, 159–178. doi:10.1016/j.precamres.2018.08.013

Hanžl, P., Melichar, R., 1997. The Brno Massif, a section through the active continental margin of a composed terrane? Krystalinikum, 23, 33–58.

Hanžl, P., Janoušek, V., Soejono, I., Buriánek, D., Svojtka, M., Hrdličková, K., Erban, V., Pin, C., 2019. The rise of the Brunovistulicum, age, geology, petrology and geochemical character of the Neoproterozoic magmatic rocks of the Central Basic Belt of the Brno Massif. Int. J. Earth Sci. 108, 1165–1199. doi: 10.1007/s00531-019-01700-2

Hanžl, P., Janoušek, V., Žáček, V., Wilimský, D., Aichler, J., Erban, V., Pudilová, M., Chlupáčová, M., Buriánková, K., Mixa, P., Pecina, V., 2007b. Magmatic history of granite-derived mylonites from the southern Desná Unit (Silesicum, Czech Republic). Miner. Petrol. 89, 45–75. doi: 10.1007/s00710-006-0137-5

Hartley, A.J., Otava, J., 2001. Sediment provenance and dispersal in a deep marine foreland basin: the Lower Carboniferous Culm Basin, Czech Republic. J. Geol. Soc. London. 158, 137–150. doi: 10.1144/jgs.158.1.137

Hawkesworth, C. J., Kemp, A. I. S., 2006. Evolution of the continental crust. Nature, 443. 811–817. doi: 10.1038/nature05191

Henderson, B.J., Collins, W.J., Murphy, J.B., Gutierrez-Alonso, G., Hand, M., 2016. Gondwanan basement terranes of the Variscan–Appalachian orogen: Baltican, Saharan and West African hafnium isotopic fingerprints in Avalonia, Iberia and the Armorican Terranes. Tectonophysics, 681, 278–304. doi:10.1016/j.tecto.2015.11.020

Hladil, J., Mazur, S., Galle, A., Ebert, J. R., 1999. Revised age of the Mały Bożków limestone in the Kłodzko metamorphic unit (early Givetian, late Middle Devonian) implications for the geology of the Sudetes, SW Poland. Neues Jahrb. fur Geol. Palaontol. Abh. 54, 329–353.doi: 10.1127/njgpa/211/1999/329

Höck, V., Montag, O., Leichmann, J., 1997. Ophiolite remnants at the eastern margin of the Bohemian Massif and their bearing on the tectonic evolution. Miner. Petrol. 60. 267–287. doi: 10.1007/BF01173712

Hoffman, P.F., 1991. Did the Breakout of Laurentia Turn Gondwanaland Inside-Out ? Science, 252, 1409–1412. doi: 10.1126/science.252.5011.1409

Ibanez-Mejia, M., Pullen, A., Arenstein, J., Gehrels, G.E., Valley, J., Ducea, M.N., Mora, A.R., Pecha, M., Ruiz, J., 2015. Unraveling crustal growth and reworking processes in complex zircons from orogenic lower-crust: The Proterozoic Putumayo Orogen of Amazonia. Precambrian Res. 267, 285–310. doi:10.1016/j.precamres.2015.06.014

Jackson, L.J., Horton, B.K., Vallejo, C., 2019. Detrital zircon U-Pb geochronology of modern Andean rivers in Ecuador: Fingerprinting tectonic provinces and assessing downstream propagation of provenance signals. Geosphere, 15, 1943–1957. doi:10.1130/GES02126.1

Jackson, S.E., Pearson, N.J., Griffin, W.L., Belousova, E.A. ,2004. The application of laser ablation-inductively coupled plasma-mass spectrometry to in situ U–Pb zircon geochronology. Chem. Geol. 211, 47–69. doi: 10.1016/j.chemgeo.2004.06.017

Janoušek, V., 2006. Saturnin, R language script for application of accessory-mineral saturation models in igneous geochemistry. Geol. Carpath. 57, 131–142.

Janoušek, V., Aichler, J., Hanžl, P., Gerdes, A., Erban, V., Pecina, V., Žáček, V., Pudilová, M., Hrdličková, K., Mixa, P., Žáčková, E., 2014. Constraining genesis and geotectonic setting of metavolcanic complexes, a multidisciplinary study of the Devonian Vrbno Group (Hrubý Jeseník Mts., Czech Republic). Int. J. Earth Sci. 103, 455–483. doi: 10.1007/s00531-013-0975-4

Jastrzębski, M., Zelażniewicz, A., Majka, J., Murtezi, M., Bazarnik, J., Kapitonov, I., 2013. Constraints on the Devonian-Carboniferous closure of the Rheic Ocean from a multi-method geochronology study of the Staré Město Belt in the Sudetes (Poland and the Czech Republic). Lithos, 170–171, 54–72. doi:10.1016/j.lithos.2013.02.021

Jastrzębski, M., Żelaźniewcz, A., Sláma, J., Machowiak, K., Śliwiński, M., Jaźwa, A., Kocjan, I., 2021. Provenance of Precambrian basement of the Brunovistulian Terrane: New data from its Silesian part (Czech Republic, Poland), central Europe, and implications for Gondwana break-up. Precambrian Res. 355, 106–108. doi:10.1016/j.precamres.2021.106108

Jelínek, E., Dudek, A., 1993. Geochemistry of the subsurface Precambrian plutonic rocks from the Brunovistulian complex in the Bohemian massif, Czechoslovakia. Precambrian Res. 62, 103–125. doi: 10.1016/0301-9268(93)90096-K

Kalvoda, J., Bábek, O., Fatka, O., Leichmann, J., Melichar, R., Nehyba, S., Špaček, P., 2008. Brunovistulian Terrane (Bohemian Massif, Central Europe) from late Proterozoic to late Paleozoic, a review. Int. J. Earth Sci. 97, 497–518. doi: 10.1007/s00531-007-0183-1

Kettner, R., Remes, M., 1936. Auffindung von silurischen Schiefern mit einer Graptolithenfauna in Mähren. Zbl. Mineral. Geol. Paläont. Abt. B1, 21–26.

Kirkland, C.L., Bingen, B., Whitehouse, M.J., Beyer, E., Griffin, W.L., 2011. Neoproterozoic palaeogeography in the North Atlantic Region: Inferences from the Akkajaure and Seve Nappes of the Scandinavian Caledonides. Precambrian Res. 186, 127–146. doi:10.1016/j.precamres.2011.01.010

Klimas, K., Kryza, R, Fanning, C.M., 2009. Palaeo- to Mesoproterozoic inheritance and Ediacaran anatexis recorded in gneisses at the NE margin of the Bohemian Massif: SHRIMP zircon data from the Nowolesie gneiss, Fore-Sudetic Block (SW Poland). Geol. Sudet. 41, 25–42.

Konopásek, J., Hoffmann, K.-H., Sláma, J., Košler, J., 2017. The onset of flysch sedimentation in the Kaoko Belt (NW Namibia) – Implications for the pre-collisional evolution of the Kaoko–Dom Feliciano–Gariep orogen. Precambrian Res. 298, 220–234. doi: 10.1016/j.precamres.2017.06.017

Konopásek, J., Schulmann, K., Johan, V., 2002. Eclogite-facies metamorphism at the eastern margin of the Bohemian Massif—subduction prior to continental underthrusting?. Eur. J. Mineral. 14(4). 701–713. doi: 10.1127/0935-1221/2002/0014-0701

Kossmat, F., 1927. Gliederung des varistischen Gebirgsbaues: Abhandlungen Sächsischen Geologischen Landesamts. 1.

Košler, J., Konopásek, J., Sláma, J., Vrána, S., 2014. U–Pb zircon provenance of Moldanubian metasediments in the Bohemian Massif. J. Geol. Soc. London. 1711, 83–95. doi: 10.1144/jgs2013-059

Kröner, A., Štípská, P., Schulmann, K., Jaeckel, P., 2000. Chronological constrains on the pre-Variscan evolution of the northeastern margin of the Bohemian Massif, Czech Republic. In, Franke, W., Haak, V., Oncken,O., Tanner, D., (Eds.), Orogenic Processes, Quantification and Modelling in the Variscan Fold Belt. Geol. Soc. Spec. Publ. 179, 175–197. doi: 10.1144/GSL.SP.2000.179.01.12

Krzywiec, P., Poprawa, P., Mikołajczak, M., Mazur, S., Malinowski, M., 2018. Deeply concealed half-graben at the SW margin of the East European Craton (SE Poland) — Evidence for Neoproterozoic rifting prior to the break-up of Rodinia. J. Palaeogeogr. 7, 88–97. doi:10.1016/j.jop.2017.11.003

Kuznetsov, N.B., Natapov, L.M., Belousova, E.A., O'Reilly, S.Y., Griffin, W.L., 2010. Geochronological, geochemical and isotopic study of detrital zircon suites from late Neoproterozoic clastic strata along the NE margin of the East European Craton: Implications for plate tectonic models. Gondwana Res. 17, 583–601. doi:10.1016/j.gr.2009.08.005

Kuznetsov, N.B., Meert, J.G., Romanyuk, T. V., 2014. Ages of detrital zircons (U/Pb, LA-ICP-MS) from the Latest Neoproterozoic-Middle Cambrian(?) Asha Group and Early Devonian Takaty Formation, the Southwestern Urals: A test of an Australia-Baltica connection within Rodinia. Precambrian Res. 244, 288–305. doi:10.1016/j.precamres.2013.09.011

Pertoldová, J., Košuličová, M., Verner, K., Žáčková, E., Pertold, Z., Konopásek, J., Veselovský, F., Košer, J., 2014. Geochronology and petrology of pyroxene-garnet skarns (eastern Bohemian Massif): Implications for the source and evolution of the Variscan continental crust. J. Geosci. 59, 367–388. doi:10.3190/jgeosci.181

Pharaoh, T.C., 1999. Palaezoic terranes and their lithospheric boundaries within the Trans-European Suture Zone (TESZ): a review. Tectonophysics, 314, 17–41. doi.org/10.1016/S0040-1951(99)00235-8

Lancaster, P.J., Storey, C.D., Hawkesworth, C.J., Dhuime, B., 2011. Understanding the roles of crustal growth and preservation in the detrital zircon record. Earth Planet. Sci. Lett. 305, 405–412. doi:10.1016/j.epsl.2011.03.022

Li, Z.X., Bogdanova, S.V, Collins, A.S., Davidson, A., De Waele, B., Ernst, R.E., Fitzsimons, I.C.W., Fuck, R.A., Gladkochub, D.P., Jacobs, J., Karlstrom, K.E., 2008. Assembly , configuration , and break-up history of Rodinia : A synthesis. Precambrian Res. 160, 179–210. doi:10.1016/j.precamres.2007.04.021

Lindner, M., Dörr, W., Hauzenberger, C.A., Reither, D., Finger, F., 2021. In search of the oldest rock of Austria: The Hauergraben Gneiss, a 1.40 Ga old mafic quartz-monzonitic inlayer in the Dobra Gneiss (Drosendorf Unit, Bohemian Massif) as a new candidate. Austrian J. Earth Sci. 114, 29–45. doi:10.17738/ajes.2021.0002

Lindner, M., Dörr, W., Reither, D., Finger, F., 2020. The Dobra Gneiss and the Drosendorf Unit in the south-eastern Bohemian Massif, Austria: West-Amazonian crust in the heart of Europe. Geol. Soc. Spec. Publ. 503, 185–207. doi.org/10.6084/m9.figshare.c.4940946.v3

Lindner, M., Finger, F., 2018. Geochemical characteristics of the late proterozoic spitz granodiorite gneiss in the drosendorf unit (Southern Bohemian Massif, Austria) and implications for regional tectonic interpretations. J. Geosci. (Czech Republic) 63, 345–362. doi:10.3190/jgeosci.271

Linnemann, U., Gerdes, A., Hofmann, M., Marko, L., 2014. The Cadomian Orogen: Neoproterozoic to Early Cambrian crustal growth and orogenic zoning along the periphery of the West African Craton-Constraints from U-Pb zircon ages and Hf isotopes (Schwarzburg Antiform, Germany). Precambrian Res. 244, 236–278. doi:10.1016/j.precamres.2013.08.007

Linnemann, U., McNaughton, N.J., Romer, R.L., Gehmlich, M., Drost, K., Tonk, C., 2004. West African provenance for Saxo-Thuringia (Bohemian Massif): Did Armorica ever leave pre-Pangean Gondwana? - U/Pb-SHRIMP zircon evidence and the Nd-isotopic record. Int. J. Earth Sci. 93, 683–705. doi:10.1007/s00531-004-0413-8

Ludwig, K.R., 2008. User's manual for Isoplot v. 3.7, a geochronological toolkit for Microsoft Excel. Berkeley Geochronological Center Special Publications 4.

Machek, M., Soejono, I., Sláma, J., Žáčková, E., 2021. Timing and kinematics of the Variscan orogenic cycle at the Moldanubian periphery of the central Bohemian Massif. J. Geol. Soc. London. jgs2021–096. doi:10.1144/jgs2021-096

Matte, P., 1986. Tectonics and plate tectonics model for the Variscan belt of Europe. Tectonophysics, 126, 329–374. doi: 10.1016/0040-1951(86)90237-4

Matteini, M., Dantas, E.L., Pimentel, M.M., de Alvarenga, C.J.S., Dardenne, M.A., 2012. U–Pb and Hf isotope study on detrital zircons from the Paranoá Group, Brasília Belt Brazil: Constraints on depositional age at Mesoproterozoic–Neoproterozoic transition and tectono-magmatic events in the São Francisco craton. Precambrian Res. 206–207, 168–181. doi:10.1016/j.precamres.2012.03.007

Martínez Catalán, J.R., 2011. Are the oroclines of the Variscan belt related to late Variscan strike-slip tectonics? Terra Nov. 23, 241–247. doi:10.1111/j.1365-3121.2011.01005.x

Martínez Catalán, J.R., Collett, S., Schulmann, K., Aleksandrowski, P., Mazur, S., 2020. Correlation of allochthonous terranes and major tectonostratigraphic domains between NW Iberia and the Bohemian Massif, European Variscan belt. Int. J. Earth Sci. 109, 1105–1131. doi:10.1007/s00531-019-01800-z

Matura, A., 2003. Zur tektonischen Gliederung der variszischen Metamorphite im Waldviertel Niederösterreichs. Jb. Geol. BA. 143. 221–225.

Mazur, S., Szczepański, J., Turniak, K., Mcnaughton, N.J., 2012. Location of the Rheic suture in the eastern Bohemian Massif: Evidence from detrital zircon data. Terra Nov. 24, 199–206. doi:10.1111/j.1365-3121.2011.01053.x

Mazur, S., Kröner, A., Szczepański, J., Turniak, K., Hanžl, P., Melichar, R., Rodionov, N.V., Paderin, I., Sergeev, S.A., 2010. Single zircon U-Pb ages and geochemistry of granitoid gneisses from SW Poland, evidence for an Avalonian affinity of the Brunian microcontinent. Geological Magazine, 147, 508–526. doi:10.1017/S001675680999080X

Mazur, S., Mikolajczak, M., Krzywiec, P., Malinowski, M., Buffenmyer, V., Lewandowski, M., 2015. Is the Teisseyre-Tornquist Zone an ancient plate boundary of Baltica? Tectonics, 34, 2465–2477. doi: 10.1002/2015TC003934

Mazur, S., Porębski, S.J., Kędzior, A., Paszkowski, M., Podhalańska, T., Poprawa, P., 2018. Refined timing and kinematics for Baltica–Avalonia convergence based on the sedimentary record of a foreland basin. Terra Nov. 30, 8–16. doi:10.1111/ter.12302

McGee, B., Collins, A.S., Trindade, R.I.F., Payne, J., 2015. Age and provenance of the Cryogenian to cambrian passive margin to foreland basin sequence of the northern Paraguay Belt, Brazil. Bull. Geol. Soc. Am. 127, 76–86. doi:10.1130/B30842.1

McLelland, J.M., Selleck, B.W., Bickford, M.E., 2010. Review of the Proterozoic evolution of the Grenville Province, its Adirondack outlier, and the Mesoproterozoic inliers of the Appalachians. In: Tollo, R.P., Bartholomew, M.J., Hibbard, J.P., Karabinos, P.M., (eds) From Rodinia to Pangea: the Lithotectonic Record of the Appalachian Region. Geol. Soc. Amer. Memoir. 206, 21–49.

Meinhold, G., Morton, A.C., Avigad, D., 2013. New insights into peri-Gondwana paleogeography and the Gondwana super-fan system from detrital zircon U–Pb ages. Gondwana Res. 23, 661–665. doi:10.1016/j.gr.2012.05.003

Miller, C.F., McDowell, S.M., Mapes, R.W., 2003. Hot and cold granites? Implications of zircon saturation temperatures and preservation of inheritance. Geology, 31, 529–532. doi:10.1130/0091-7613(2003)031<0529:HACGIO>2.0.CO;2

Moczydlowska, M., 1997. Proterozoic and Cambrian successions in Upper Silesia, an Avalonian terrane in southern Poland. Geological Magazine, 134, 679–689. doi:10.1017/S0016756897007504

Moores, E.M., 1981. Ancient Suture Zones within Continents. Science, 213, 41–46. doi: 10.1126/science.213.4503.41

Murphy, J.B., Pisarevsky, S.A., Nance, R.D., Keppie, J.D., 2004. Neoproterozoic–Early Paleozoic evolution of peri-Gondwanan terranes: implications for Laurentia–Gondwana connections. Int. J. Earth. Sci. 93, 659–682. doi: 10.1007/s00531-004-0412-9

Nance, R.D., Murphy, J.B., 1994. Constraining basement isotopic signatures and the palinspastic restoration of peripheral orogens: example from the Neoproterozoic Avalonian–Cadomian belt. Geology, 22, 617–620. doi:10.1130/0091-7613(1994)022<0617:CBISAT>2.3.CO;2

Nance, R.D., Gutiérrez-Alonso, G., Keppie, J.D., Linnemann, U., Murphy, J.B., Quesada, C., Strachan, R. a., Woodcock, N.H., 2010. Evolution of the Rheic Ocean. Gondwana Res.

17, 194–222. doi:10.1016/j.gr.2009.08.001

Nance, R.D., Murphy, J.B., Strachan, R.A., D'Lemos, R.S., Taylor, G.K., 1991. Late Proterozoic tectonostratigraphic evolution of the Avalonian and Cadomian terranes. Precambrian Res. 53, 41–78. doi: 10.1016/0301-9268(91)90005-U

Nawrocki, J., Żylińska, A., Buła, Z., Grabowski, J., Krzywiec, P., Poprawa, P., 2004. Early Cambrian location and affinities of the Brunovistulian terrane (Central Europe) in the light of palaeomagnetic data. Geol. Soc. Spec. Publ. 161, 513–522. doi: 10.1144/0016-764903-083

Nawrocki, J., Leichmann, J., Pańczyk, M., 2021. Mid-Ediacaran bimodal magmatism and peri-Baltic affinity of the Brunovistulian terrane documented by the U-Pb isotope and palaeomagnetic data from the Brno Massif (Central Europe). Precambrian Res. 358. 106–147. doi:10.1016/j.precamres.2021.106147

Oberc-Dziedzic, T., Klimas K, Kryza, R., Fanning, C.M., 2003. SHRIMP U–Pb zircon geochronology of the Strzelin gneiss, SW Poland: evidence for a Neoproterozoic thermal event in the Fore-Sudetic Block, Central European Variscides. Int. J. Earth. Sci. 92, 701–711. doi: 10.1007/s00531-003-0345-8

Oberc-Dziedzic, T., Pin, C., Madej, S., Kryza, R., 2021. Reconstruction of the thermal history of the northwestern part of the Brunovistulicum. Int. J. Earth Sci. 110, 2091–2114. doi:10.1007/s00531-021-02061-5

Oriolo, S., Schulz, B., Geuna, S., González, P.D., Otamendi, J.E., Sláma, J., Druguet, E., Siegesmund, S., 2020. Early Paleozoic accretionary orogens along the Western Gondwana margin. Geosci. Front. 12, 109–130. doi:10.1016/j.gsf.2020.07.001

Paszkowski, M., Budzyń, B., Mazur, S., Sláma, J., Środoń, J., Millar, I. L., Shumlyanskyy, L., Kędzior, A., Liivamägi, S., 2021. Detrital zircon U–Pb and Hf constraints on provenance and timing of deposition of the Mesoproterozoic to Cambrian sedimentary cover of the East European Craton, part II: Ukraine. Precambrian Res. 362, 106282. doi: 10.1016/j.precamres.2021.106282

Percival, J.J., Konopásek, J., Eiesland, R., Sláma, J., de Campos, R. S., Battisti, M. A., Bitencourt, M. d. F., 2021. Pre-orogenic connection of the foreland domains of the Kaoko–Dom Feliciano–Gariep orogenic system. Precambrian Res. 354, 106060. doi: 10.1016/j.precamres.2020.106060

Pettersson, C.H., Pease, V., Frei, D., 2009. U-Pb zircon provenance of metasedimentary basement of the Northwestern Terrane, Svalbard: Implications for the Grenvillian-Sveconorwegian orogeny and development of Rodinia. Precambrian Res. 175, 206–220. doi:10.1016/j.precamres.2009.09.010

Pharaoh, T. C., 1999. Palaeozoic terranes and their lithospheric boundaries within the Trans-European Suture Zone (TESZ): a review. Tectonophysics, 314, 17–41. doi: 10.1016/S0040-1951(99)00235-8

Poprawa, P., 2019. Geological setting and Ediacaran–Palaeozoic evolution of the western slope of the East European Craton and adjacent regions. An. Soc. Geol. Pol. 89, 347–380. doi:10.14241/asgp.2019.23

Poprawa, P., Krzemińska, E., Paczeŝna, J., Amstrong, R., 2020. Geochronology of the Volyn volcanic complex at the western slope of the East European Craton – Relevance to the Neoproterozoic rifting and the break-up of Rodinia/Pannotia. Precambrian Res. 346, 105817. doi:10.1016/j.precamres.2020.105817

Racek, M., Lexa, O., Schulmann, K., Corsini, M., Štípská, P., Maierová, P., 2017. Re-evaluation of polyphase kinematic and 40Ar/39Ar cooling history of Moldanubian hot nappe at the eastern margin of the Bohemian Massif. Int. J. Earth Sci. 106, 397–420.

doi:10.1007/s00531-016-1410-4

Samson, S.D., D'Lemos, R.S., Miller, B. V. & Hamilton, M. A. 2005. Neoproterozoic palaeogeography of the Cadomia and Avalon terranes: constraints from detrital zircon U–Pb ages. J. Geol. Soc. London. 162, 65–71. https://doi.org/10.1144/0016-764904-003

Saylor, J.E., Knowles, J.N., Horton, B.K., Nie, J., Mora, A., 2013. Mixing of source populations recorded in detrital zircon U–Pb age spectra of modern river sands. J. Geol. 121, 17–33. doi:10.1086/668683

Scotese, C.R., 2009. Late Proterozoic plate tectonics and palaeogeography: a tale of two supercontinents, Rodinia and Pannotia. Geol. Soc. London, Spec. Publ. 326, 67–83. doi:10.1144/SP326.4

Schaltegger, U., Schmitt, A.K., Horstwood, M.S.A., 2015. U–Th–Pb zircon geochronology by ID-TIMS, SIMS, and laser ablation ICP-MS: Recipes, interpretations, and opportunities. Chem. Geol. 402, 89–110. doi:10.1016/j.chemgeo.2015.02.028

Schulmann, K., Kröner, A., Hegner, E., Wendt, I., Konopásek, J., Lexa, O., Štípská, P., 2005. Chronological constraints on the pre-orogenic history, burial and exhumation of deep-seated rocks along the eastern margin of the Variscan orogen, Bohemian Massif, Czech Republic. Am. J. Sci. 305. 407–448. doi:10.2475/ajs.305.5.407

Schulmann, K., Konopásek, J., Janoušek, V., Lexa, O., Lardeaux, J.M., Edel, J.B., Štípská, P., Ulrich, S., 2009. An Andean type Palaeozoic convergence in the Bohemian Massif. Comptes Rendus Geoscience, 341, 266–286. doi:10.1016/j.crte.2008.12.006

Schulmann, K., Ledru, P., Autran, A., Melka, R., Lardeaux, J.M., Urban, M., Lobkowicz, M., 1991. Evolution of nappes in the eastern margin of the Bohemian Massif, a kinematic interpretation. Geol. Rundsch. 80, 73–92. doi:10.1007/BF01828768

Schulmann, K., Lexa, O., Janoušek, V., Lardeaux, J.M., Edel, J.B., 2014b. Anatomy of a diffuse cryptic suture zone: An example from the Bohemian Massif, European variscides. Geology, 42, 275–278. doi:10.1130/G35290.1

Schulmann, K., Martelat, J.E., Ulrich, S., Lexa, O., Štípská, P., Becker, J.K., 2008. Vertical extrusion and horizontal channel flow of oro- genic lower crust: key exhumation mechanisms in large hot orogens? J. Metamorph. Geol. 26, 273–297. doi.org/10.111 1/j.1525-1314.2007.00755 .x

Schulmann, K., Martínez Catalán, J.R., Lardeaux, J.M., Janoušek, V., Oggiano, G., 2014b. The Variscan Orogeny, extent, timescale and the formation of the European crust. In, Schulmann, K., Martínez Catalán, J.R., Lardeaux, J.M., Janoušek, V., Oggiano, G., (eds) The Variscan Orogeny, Extent, Timescale and the Formation of the European Crust. Geol. Soc. Spec. Publ. 405, 1–6, doi:10.1144/SP405.15

Scherer, E., Münker, C., Mezger, K., 2001. Calibration of the Lutetium–Hafnium clock. Science, 293, 683–687. doi:10.1126/science.1061372

Shumlyanskyy, L., Nosova, A., Billstrom, K., Soderlund, U., Andreasson, P.-G., Kuzmenkova, O., 2016. The U-Pb zircon and baddeleyite ages of the Neoproterozoic Volyn Large Igneous Province: implication for the age of the magmatism and the nature of a crustal contaminant. GFF 138 (1), 17–30. doi:10.1080/11035897.2015.1123289

Singh, M., Singh, I.B., Müller, G., 2007. Sediment characteristics and transportation dynamics of the Ganga River. Geomorphology, 86, 144–175. doi:10.1016/j.geomorph.2006.08.011

Sláma, J., 2016. Rare late Neoproterozoic detritus in SW Scandinavia as a response to distant tectonic processes. Terra Nov. 28, 394–401. doi:https://doi.org/10.1111/ter.12232

Sláma, J., Dunkley, D.J., Kachlík, V., Kusiak, M.A., 2008a. Transition from island-arc to passive setting on the continental margin of Gondwana: U–Pb zircon dating of Neoproterozoic metaconglomerates from the SE margin of the Teplá–Barrandian Unit. Bohemian Massif, Tectonophysics, 461, 44–59. doi:10.1016/j.tecto.2008.03.005

Sláma, J., Košler, J., Condon, D.J., Crowley, J.L., Gerdes, A., Hanchar, J.M., Horstwood, M.S.A., Morris, G.A., Nasdala, L., Norberg, N., Schaltegger, U., Schoene, B., Tubrett, M.N., Whitehouse, M.J., 2008b. Plešovice zircon – a new natural reference material for U–Pb and Hf isotopic microanalysis. Chemic. Geol. 249, 1–35. doi: 10.1016/j.chemgeo.2007.11.005

Soejono, I., Janoušek, V., Žáčková, E., Sláma, J., Konopásek, J., Machek, M., Hanžl, P., 2017. Long-lasting Cadomian magmatic activity along an active northern Gondwana margin, U–Pb zircon and Sr–Nd isotopic evidence from the Brunovistulian Domain, eastern Bohemian Massif. Int. J. Earth. Sci. 106, 2109–2129. doi:10.1007/s00531-016-1416-y

Soejono, I., Machek, M., Sláma, J., Janoušek, V., Kohút, M., 2020. Cambro-Ordovician anatexis and magmatic recycling at the thinned Gondwana margin: new constraints from the Kouřim Unit, Bohemian Massif. J. Geol. Soc. London. 177, 325–341. doi:10.1144/jgs2019-037

Soejono, I., Žáčková, E., Janoušek, V., Machek, M., Košler, J., 2010. Vestige of an Early Cambrian incipient oceanic crust incorporated in the Variscan orogen, Letovice Complex, Bohemian Massif. J. Geol. Soc. London. 167, 1113–1130. doi: 10.1144/0016-76492009-180

Sorger, D., Hauzenberger, C.A., Finger, F., Linner, M., 2020. Two generations of Variscan garnet: Implications from a petrochronological study of a high-grade Avalonia-derived paragneiss from the Drosendorf unit, Bohemian Massif. Gondwana Res. 85, 124–148. doi:10.1016/j.gr.2020.04.004

Stephan, T., Kroner, U., Romer, R.L., 2019. The pre-orogenic detrital zircon record of the Peri-Gondwanan crust. Geol. Mag. 156, 281–307. doi:10.1017/S0016756818000031

Suess, F.E., 1912. Die moravische Fenster und ihre Beziehung zum Grundgebirge des Hohen Gesenkes. Denkschriften Österreichische Akademie der Wissenschaften, Mathematisch-naturwissenschaftliche Klasse, 88, 541–631.

Suess, F. E., 1926. Intrusionstektonik u. Wandertektonick im variszischeu Grundgebirge. 48–54.

Svojtka, M., Breiter, K., Ďurišová, J., Ackerman, L., Veselovský, F., Šmerda, J., 2017. Geochemistry and U–Pb zircon ages of Derflice granodiorite from the Thaya (Dyje) Massif. Geosci. Res. Rep. 50, 17–24. doi:10.3140/zpravy.geol.2017.03

Šamajová, L., Hók, J., Bielik, M., Pelech, O., 2018. Deep contact of the Bohemian Massif and Western Carpathians as seen from density modeling. Geol. Carpath. 69, 545–557. doi: 10.1515/geoca-2018-0032

Špaček, P., Kalvoda, J., 2000. Reconstruction of syn- and postsedi- mentary tectonic events in flysch basin from limestone pebbles variation: Drahany Culm of the Moravian Rhenohercynian Zone. Geol. Carpath. 51. 37–48.

Štípska, P., Hacker, B.R., Racek, M., Holder, R., Kylander-Clark, a. R.C., Schulmann, K., Hasalová, P., 2015. Monazite Dating of Prograde and Retrograde P-T-d paths in the Barrovian terrane of the Thaya window, Bohemian Massif. J. Petrol. 56, 1007–1035. doi:10.1093/petrology/egv026

Štípská, P., Pitra, P., Powell, R., 2006. Separate or shared metamorphic histories of eclogites and surrounding rocks? An example from the Bohemian Massif. J. Metamorph. Geol.

24, 219–240. doi:10.1111/j.1525-1314.2006.00634.x

Štípská, P., Schulmann, K., Powell, R., 2008. Contrasting metamorphic histories of lenses of high-pressure rocks and host mig- matites with a flat orogenic fabric (Bohemian Massif, Czech Republic): a result of tectonic mixing within horizontal crustal flow? J. Metamorph. Geol. 26, 623–646. doi: 10.111 1/j.1525-1314.2008.00781 .x

Štípská, P., Schulmann, K., Racek, M., Lardeaux, J.M., Hacker, B.R., Kylander-Clark, A.R.C., Holder, R., Košuličová, M., 2020. Finite pattern of Barrovian metamorphic zones: interplay between thermal reequilibration and post-peak deformation during continental collision—insights from the Svratka dome (Bohemian Massif). Int. J. Earth Sci. 109, 1161–1187. doi:10.1007/s00531-019-01788-6

Tabaud, A.S., Štípská, P., Mazur, S., Schulmann, K., Míková, J., Wong, J., Sun, M., 2021. Evolution of a Cambro-Ordovician active margin in northern Gondwana: Geochemical and zircon geochronological evidence from the Góry Sowie metasedimentary rocks, Poland. Gondwana Res. 90, 1–26. doi:10.1016/j.gr.2020.10.011

Tassinari, C.C.G., Macambira, M.J.B., 1999. Geochronological provinces of the Amazonian Craton. Episodes, 22, 174–182. Doi: 10.18814/epiiugs/1999/v22i3/004

Teixeira, W., Tassinari, C.C.G., Cordani, U.G., Kawashita, K., 1989. A review of the geochronology of the Amazonian craton: Tectonic implications. Precambrian Res. 42, 213–227. doi:10.1016/0301-9268(89)90012-0

Timmerman, J. M., Krmíček, L., Krmíčková, S., Sláma, J., 2019. LA-ICP-MS zircon ages of the Slavkov Terrane, Central Basic Belt and Basal Clastics, Brunovistulicum, Czech Republic. In: Hrdličková, K., Daňková, L., (eds) 17th Meeting of the Central European Tectonic Groups, CETEG 2019, Rozdrojovice, 24–27 April, 2019. Rozdrojovice, p 84.

Tomek, F., Vacek, F., Žák, J., Petronis, M.S., Verner, K., Foucher, M.S., 2019. Polykinematic foreland basins initiated during orthogonal convergence and terminated by orogen-oblique strike-slip faulting: An example from the northeastern Variscan belt. Tectonophysics, 766, 379–397. doi:10.1016/j.tecto.2019.05.023

Trubač, J., Janoušek, V., Vrána, S., Wiegand, B., 2012. Nature , tectonic setting and likely origin of the Paleoproterozoic (~ 2.1 Ga) Světlík orthogneisses (southern Bohemia). Miner. Slov. 44, 110.

Trubač, J., Žák, J., Chlupáčová, M., Janoušek, V., 2009. Magnetic fabric of the Říčany granite, Bohemian Massif: A record of helical magma flow?. J. Volcan. Geoth. Res. 181, 25–34. doi:10.1016/j.jvolgeores.2008.12.005

van Breemen, O., Aftalion, M., Bowes, D.R., Dudek, A., Mísař, Z., Povondra, P., Vrána, S., 1982. Geochronological studies of the Bohemian Massif, Czechoslovakia, and their significance in the evolution of Central Europe. Trans. R. Soc. Edinb. 73, 89–108. doi:10.1017/S0263593300009639

Vavrdová, M., Mikuláš, R., Nehyba, S., 2003. Lower Cambrian siliciclastic sediments in southern Moravia (Czech Republic) and their paleogeographical constraints. Geol. Carpath. 54, 67–79.

von Raumer, J.F., Stampfli, G., Borel, G. & Bussy, F. 2002. Organization of pre-Variscan basement areas at the north-Gondwanan margin. Int. J. Earth Sci. 91. 35–52. doi: 10.1007/s005310100200

Waldhausrová, J., 1984. Proterozoic volcanics and intrusive rocks of the Jílové Zone (Central Bohemia). Krystalinikum, 17, 77–97.

Watson, E.B., Harrison, T.M., 1983. Zircon saturation revisited: temperature and composition effects in a variety of crustal magma types. Earth Planet. Sci. Lett. 64, 295–304. doi: 10.1016/0012-821X(83)90211-X

Wendt, J. I., Kröner, A., Fiala, J., Todt, W., 1994. U–Pb zircon and Sm-Nd dating of Moldanubian HP/HT granulites from South Bohemia, Czech Republic. J. Geol. Soc. London. 151. 83–90. doi: 10.1144/gsjgs.151.1.0083

Wiedenbeck, M., Alle, P., Corfu, F., Griffin, W.L., Meier, M., Oberli, F., von Quadt, A., Roddick, J.C., Spiegel, W., 1995. Three natural zircon standards for U–Th–Pb, Lu–Hf, trace element and REE analyses. Geostandards Newsletters, 19. 1–23. doi: 10.1111/j.1751-908X.1995.tb00147.x

Winchester, J.A. 2002. Palaeozoic amalgamation of Central Europe: new results from recent geological and geophysical investigations. Tectonophysics, 360, 5–21. doi:10.1016/S0040-1951(02)00344-X

Zeh, A., Gerdes, A., Klemd, R., and Barton, J.M. 2007. Archaean to proterozoic crustal evolution in the central zone of the limpopo belt (south africa-botswana): Constraints from combined U–Pb and Lu–Hf isotope analyses of zircon. J. Petrol. 48, 1605–1639. doi: 10.1093/petrology/egm032

Zhang, W., Roberts, D., Pease, V., 2015. Provenance characteristics and regional implications of Neoproterozoic, Timanian-margin successions and a basal Caledonian nappe in northern Norway. Precambrian Res. 268, 153–167. doi:10.1016/j.precamres.2015.07.006

Żelaźniewicz, A., Fanning, C.M., 2020. Neoarchean to paleoproterozoic fragments in the brunovistulia terrane, S Poland: A component of the Columbia supercontinent? Geol. Q. 64, 120–129. doi:10.7306/gq.1515

Źelaźniewicz, A., Buła, Z., Fanning, M., Seghedi, A., Źaba, J., 2009. More evidence on Neoproterozoic terranes in southern Poland and southeastern Romania. Geol. Q. 53, 93–124.

Żelaźniewicz, A., Oberc-Dziedzic, T., Sláma, J., 2020. Baltica and the Cadomian orogen in the Ediacaran – Cambrian : a perspective from SE Poland. Int. J. Earth Sci. doi:10.1007/s00531-020-01858-0

Žáčková, E., Konopásek, J., Košler, J., Jeřábek, P., 2012. Detrital zircon populations in quartzites of the Krkonoše-Jizera Massif: Implications for pre-collisional history of the Saxothuringian Domain in the Bohemian Massif. Geol. Mag. 149, 443–458. doi:10.1017/S0016756811000744

Žák, J., Kratinová, Z., Trubač, J., Janoušek, V., Sláma, J., Mrlina, J., 2011. Structure, emplacement, and tectonic setting of Late Devonian granitoid plutons in the Teplá-Barrandian unit, Bohemian Massif. Int. J. Earth Sci. 100, 1477–1495. doi:10.1007/s00531-010-0565-7

Žák, J., Sláma, J., 2018. How far did the Cadomian ?terranes? travel from Gondwana during early Palaeozoic? A critical reappraisal based on detrital zircon geochronology. Int. Geol. Rev. 60, 319–338. doi:10.1080/00206814.2017.1334599

Žák, J., Svojtka, M., Hajná, J., Ackerman, L., 2020. Detrital zircon geochronology and processes in accretionary wedges. Earth-Science Rev. 207, 103214. doi:10.1016/j.earscirev.2020.103214

Figure captions

Fig. 1 (a) Schematic map of the European Variscides showing preserved Cadomian basement complexes and major lithotectonic zones (modified after Martínez Catalán, 2011). (b) Simplified geological map of the Bohemian Massif (modified after Machek et al., 2021). (c) Geological map of the Brunovistulian Domain with locations of dated samples (modified after Hanžl et al., 2019).

Fig. 2 (a) Sheet-like intrusion of the western Brno Massif granodiorite within the pre-Cadomian host-rock (migmatite UD 16). Inset shows close-up view on migmatite septa within granodiorite. (b) Migmatite UD 23 intruded by granodiorite apophyses. (c) Migmatized paragneiss from the eastern margin of the Slavkov Terrane (UD 18). (d) Dated borehole core samples from the covered southeastern part of Brunovistulian Domain. (e) Quarzitic gneiss from the lowermost metasedimentary nappe of the southern Moravo–Silesian Zone (UD 11). (f) Garnetiferous micaschist UD 20 from the northern part of the Micaschist Zone.

Fig. 3 Macro- and microphotographs of representative studied samples from the (a, b) Tonian sequences, (c, d) covered Ediacaran sequences (e) Moravo–Silesian Zone and (f) Micaschist Zone.

Fig. 4 Cathodoluminescence images of typical zircons from the (a, b) Tonian sequences, (c–i) the Ediacaran sequences, (j) Moravo–Silesian Zone and (k) Micaschist Zone. Laser dating and Hf analyses spots are marked with concordant $^{206}Pb/^{238}U$ ages ± 2σ uncertainties ($^{207}Pb/^{206}Pb$ for ages > 1 Ga) and $\varepsilon_{Hf(t)}$ values with 2σ uncertainties.

Fig. 5 Frequency histograms with kernel density distributions of detrital zircon age populations for investigated metasedimentary rocks (n, number of analyses). Only data less than 10% discordant $^{206}Pb/^{238}U$ ages ($^{207}Pb/^{206}Pb$ for ages > 1 Ga) were included.

Fig. 6 Maximal depositional age of studied samples calculated as the $^{206}Pb/^{238}U$ weigted mean and concordia ages of the youngest zircon group (data-point error symbols and ellipses are 2σ).

Fig. 7 Combined U–Pb age and Hf isotopic data for detrital zircons from studied units. Grey areas represent kernel density distributions of U–Pb ages close to the Hf spot analyses and dashed lines show whole age populations. The ^{176}Lu decay constant of Scherer et al. (2001), CHUR values of Blichert-Toft and Albarède (1997), Depleted Mantle (DM) from Chauvel and Blichert-Toft (2001) and continental crust values of Zeh et al. (2007) were used.

Fig. 8 (a) Cumulative distributions of time differences between the crystallization ages (CA) and the depositional ages (DA) of detrital zircons from the studied samples of the Brunovistulian Domain. Colour fields representing different tectonic settings of deposition area after Cawood et al. (2012). (b) Comparison of the detrital zircon ages (this study and published data) from major units of the Brunovistulian Domain and the Neoproterozoic (meta-)sedimentary rocks from other parts of the Bohemian Massif. Data sources: Tonian sequences (this study), Ediacaran sequences (this study), Metasedimentary nappes of the Moravo–Silesian Zone (this study and Košler et al., 2014), Micaschist Zone (this study and Košler et al., 2014), Drosendorf Unit in Austria (Lindner et al., 2020; Sorger et al., 2020), Moldanubian Zone (Bukovská et al., 2019; Košler et al., 2014; Soejono et al., 2020), Teplá–Barrandian Unit (Drost et al., 2011; Hajná et al., 2017; Žák and Sláma, 2018).

Fig. 9 Comparison of the U–Pb detrital zircon data of studied (a) Ediacaran and (b) Tonian sequences of the Brunovistulian Domain (this study) and published data from the Neoproterozoic (meta-)sedimentary rocks of potential source areas in (c) Baltica; data from Bingen et al. (2011), Gee et al. (2014), Kirkland et al. (2011), Kuznetsov et al. (2010), Pettersson et al. (2009), Sláma (2016), Zhang et al. (2015) and Amazonia; data from Ibanez-Mejia et al. (2015), Matteini et al. (2012), McGee et al. (2015). Baltican geochronological provinces after Bogdanova et al. (2008) and Amazonian geochronological provinces after Tassinari and Macambria (1999).

Fig. 10 Comparison of combined detrital zircon age spectra ($^{206}Pb/^{238}U$ ages and $^{207}Pb/^{206}Pb$ for ages > 1 Ga) from the Brunovistulian Domain with those published from other parts of the Bohemian Massif (same data sources as in Fig. 8).

Fig. 11 Paleogeographic reconstructions showing the possible Neoproterozoic locations of the Brunovistulian Domain (modified after Cawood et al., 2016; Dalziel, 1997; Li et al., 2008), distribution of crustal sources (after Bogdanova et al., 2008 for Baltica, Tassinari and Macambria, 1999 for Amazonia and Ennih and Liégeois, 2008 for West Africa, possible sediment transport directions and detrital zircon age patterns. (a) Tonian paleogeography showing three potential locations (yellow stars) of the Brunovistulian syncollisional or extensional basin in the Rodinia interior (star 1) or in the passive margin along Rodinia exterior (stars 2 and 3). (b) Schematic cross-section for the scenario of the collisional/extensional domain in the Rodinia interior. (c) Schematic cross-section for the scenario of the Rodinia passive margin. (d) Ediacaran continental configuration with possible positions of Brunovistulian Domain (red stars) at c. 650–550 Ma. (e) Schematic cross-section of the Ediacaran active margin showing proposed position of the Brunovistulian bac-arc basin and the TBU/Mold accretionary wedge. (e) Schematic cross-section of the Ediacaran active margin. Abbreviations: BV – Brunovistulian Domain; TBU – Teplá–Barrandian Unit; Mold – Moldanubian Zone.

Table captions

Table 1 Location, petrography and summary of main age peaks of studied samples.

Sample	Latitude (N)	Longitude (E)	Regional position	Rock	MDA	Main detrital age peaks
Tonian sequences						
UD 16	49.0840500	16.5121000	host-rock of the Brno Massif (Thaya Terrane)	migmatized grt-bt paragneiss	912 ± 17 Ma	0.9–2.2 Ga, c. 2.7 Ga
UD 23	49.1475333	16.4446333	host-rock of the Brno Massif (Thaya Terrane)	migmatite	949 ± 79 Ma	0.9–1.9 Ga
Ediacaran sequences						
UD 18	50.1767333	17.3153333	Desná Dome	migmatized paragneiss	604 ± 7 Ma	c. 650 Ma, 1.8–2.5 Ga
UD 30	48.853029	16.660453	metamorphic complex of covered part of the Thaya T.	amp-bt paragneiss	579 ± 5 Ma	c. 640 Ma
UD 31	49.642432	18.714434	metamorphic complex of covered part of the Slavkov T.	migmatized paragneiss	593 ± 7 Ma	c. 620 Ma
UD 32	49.293941	17.832138	metamorphic complex of covered part of the Slavkov T.	paragneiss	602 ± 3 Ma	c. 630 Ma, 1.3–2.2 Ga
UD 33	49.577780	18.479296	metamorphic complex of covered part of the Slavkov T.	sill-bt paragneiss	555 ± 4 Ma	c. 620 Ma, 0.8–2.3 Ga
UD 34	49.077759	16.839016	metamorphic complex of covered part of the Slavkov T.	migmatized paragneiss	603 ± 5 Ma	c. 680 Ma, 1.5–2.0 Ga
UD 35	49.528029	18.517177	metamorphic complex of covered part of the Slavkov T.	amp-bt paragneiss	554 ± 4 Ma	c. 600 Ma, 1.2–2.1 Ga
Moravo-Silesian Zone						
UD 11	49.3451666	16.3401000	Svratka Dome (Bílý Potok Group)	quartzitic gneiss	550 ± 6 Ma	c. 560 Ma, 1.0–2.2 Ga, c. 2.6 Ga
Micaschist Zone						
UD 20	49.6230500	16.3597000	Micaschist Zone	grt-ms-bt micaschist	551 ± 6 Ma	c. 600 Ma, 1.8–2.4 Ga, c. 2.6 Ga

MDA - Maximum depositional age

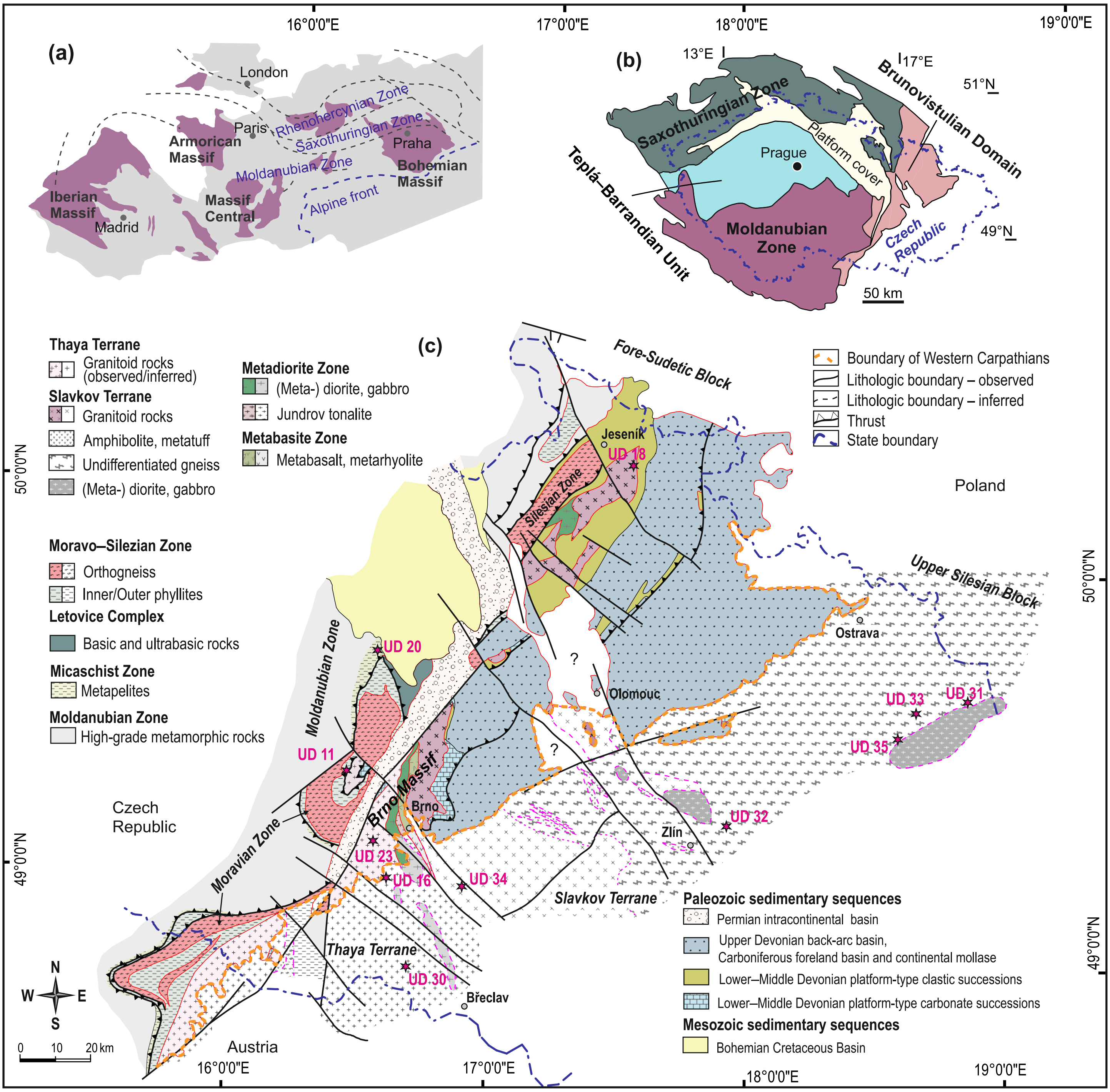

(a)
London
Paris
Rhenohercynian Zone
Saxothuringian Zone
Praha
Armorican Massif
Moldanubian Zone
Bohemian Massif
Iberian Massif
Madrid
Massif Central
Alpine front
(b)
13°E
17°E
51°N
49°N
Saxothuringian Zone
Brunovistulian Domain
Platform cover
Prague
Teplá–Barrandian Unit
Moldanubian Zone
Czech Republic
50 km
(c)
Thaya Terrane
Granitoid rocks (observed/inferred)
Slavkov Terrane
Granitoid rocks
Amphibolite, metatuff
Undifferentiated gneiss
(Meta-) diorite, gabbro
Metadiorite Zone
(Meta-) diorite, gabbro
Jundrov tonalite
Metabasite Zone
Metabasalt, metarhyolite
Moravo–Silezian Zone
Orthogneiss
Inner/Outer phyllites
Letovice Complex
Basic and ultrabasic rocks
Micaschist Zone
Metapelites
Moldanubian Zone
High-grade metamorphic rocks
Boundary of Western Carpathians
Lithologic boundary – observed
Lithologic boundary – inferred
Thrust
State boundary
Fore-Sudetic Block
Poland
Jeseník
UD 18
Silesian Zone
Upper Silesian Block
Ostrava
Olomouc
UD 33
UD 31
UD 35
UD 20
Moldanubian Zone
UD 11
Brno Massif
Brno
UD 32
Zlín
Czech Republic
Moravian Zone
UD 23
UD 16
UD 34
Slavkov Terrane
Thaya Terrane
UD 30
Břeclav
Austria
Paleozoic sedimentary sequences
Permian intracontinental basin
Upper Devonian back-arc basin, Carboniferous foreland basin and continental mollase
Lower–Middle Devonian platform-type clastic successions
Lower–Middle Devonian platform-type carbonate successions
Mesozoic sedimentary sequences
Bohemian Cretaceous Basin
16°0'0"E
17°0'0"E
18°0'0"E
19°0'0"E
50°0'0"N
49°0'0"N
N
W
E
S
0
10
20 km

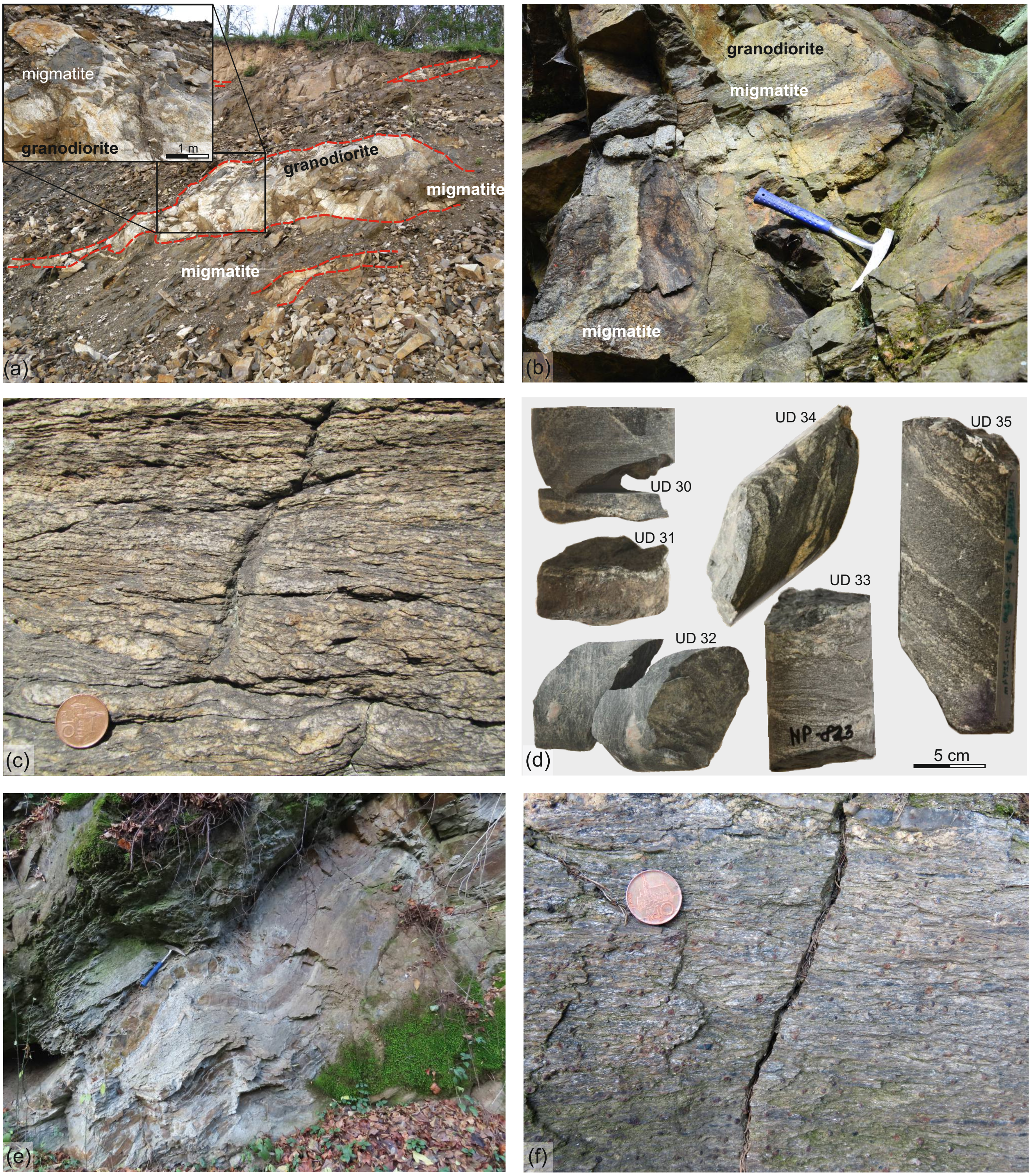
migmatite
granodiorite
1 m
granodiorite
migmatite
migmatite
(a)
granodiorite
migmatite
migmatite
(b)
(c)
UD 30
UD 34
UD 35
UD 31
UD 33
UD 32
NP-823
5 cm
(d)
(e)
(f)

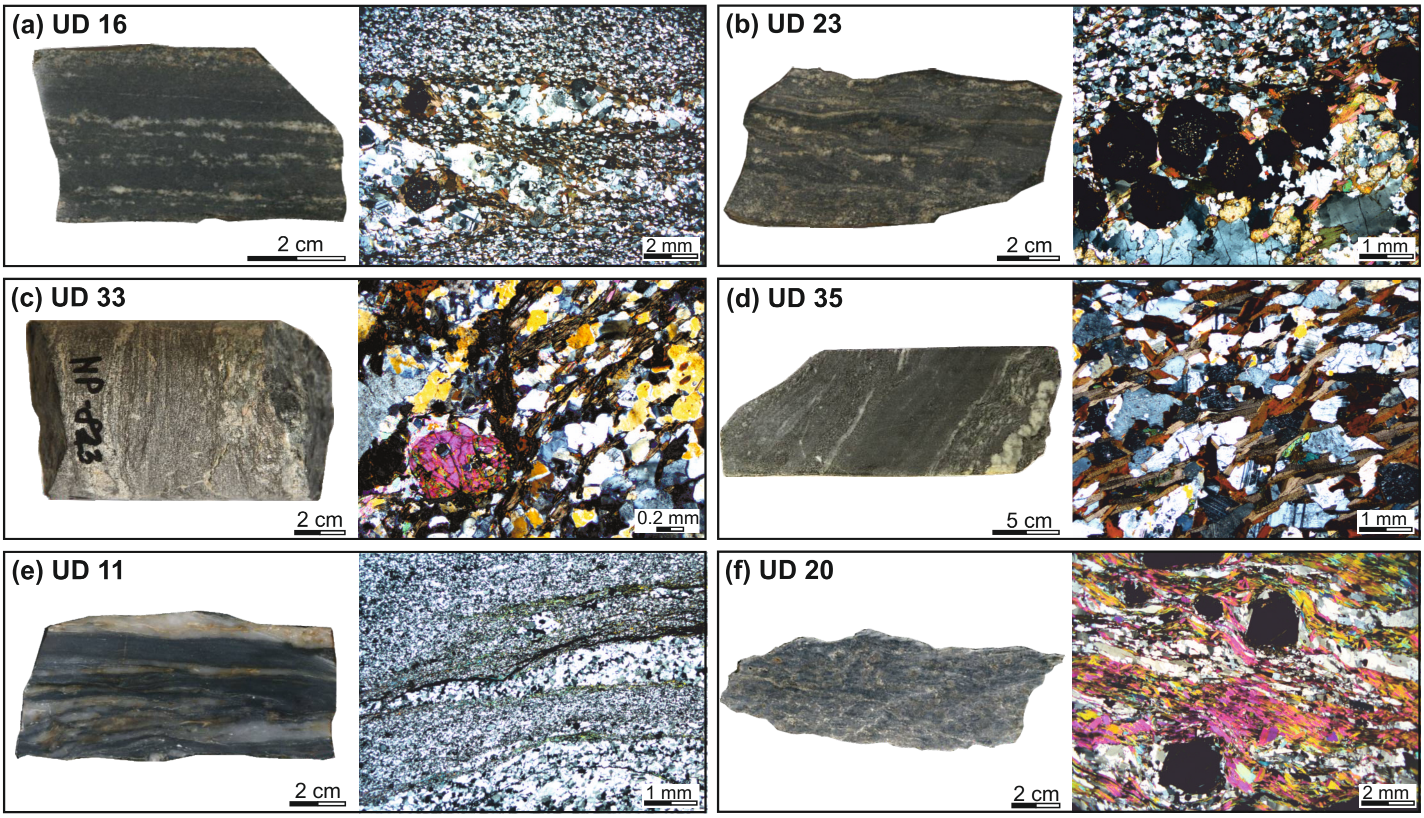

(a) UD 16
2 cm
2 mm
(b) UD 23
2 cm
1 mm
(c) UD 33
NP 23
2 cm
0.2 mm
(d) UD 35
5 cm
1 mm
(e) UD 11
2 cm
1 mm
(f) UD 20
2 cm
2 mm

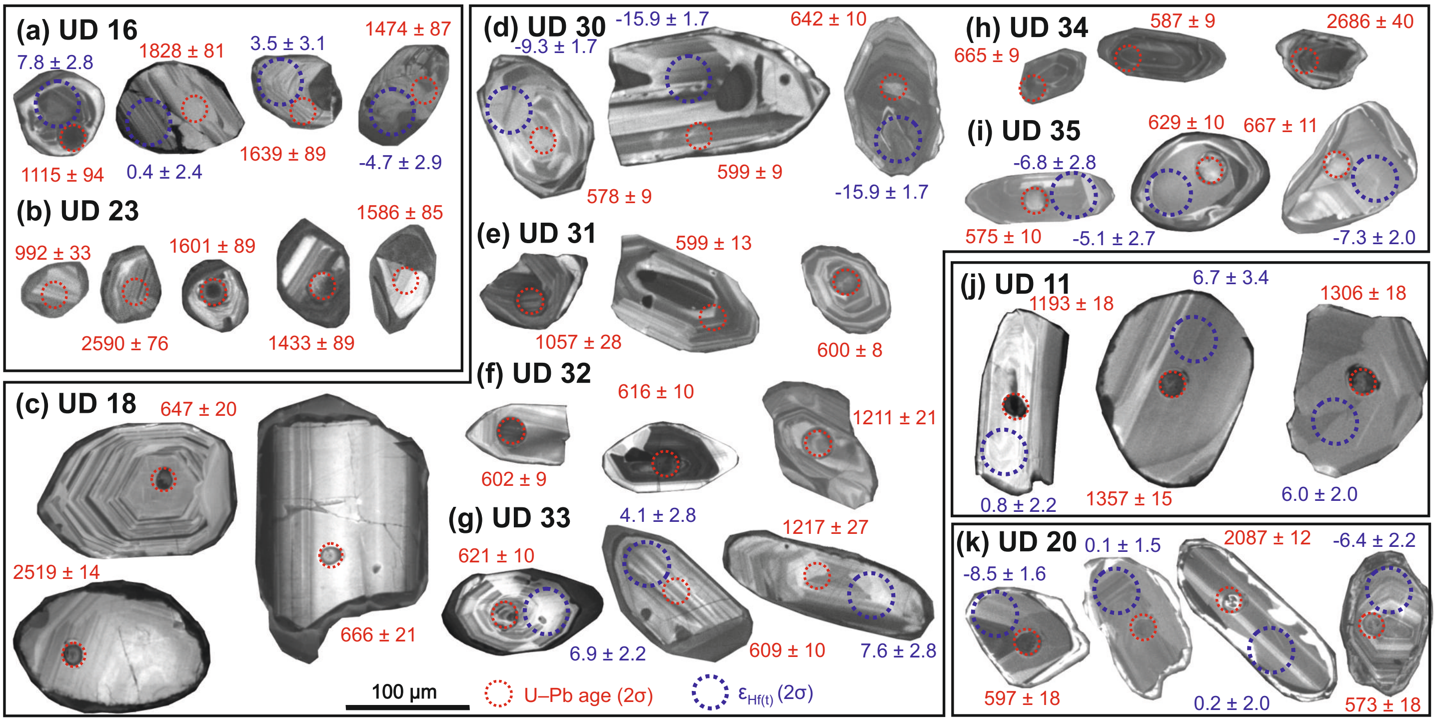
(a) UD 16
7.8 ± 2.8
1828 ± 81
3.5 ± 3.1
1474 ± 87
1115 ± 94
0.4 ± 2.4
1639 ± 89
-4.7 ± 2.9
(b) UD 23
1586 ± 85
992 ± 33
1601 ± 89
2590 ± 76
1433 ± 89
(c) UD 18
647 ± 20
2519 ± 14
666 ± 21
(d) UD 30
-15.9 ± 1.7
-9.3 ± 1.7
642 ± 10
578 ± 9
599 ± 9
-15.9 ± 1.7
(e) UD 31
599 ± 13
1057 ± 28
600 ± 8
(f) UD 32
616 ± 10
1211 ± 21
602 ± 9
(g) UD 33
4.1 ± 2.8
1217 ± 27
621 ± 10
6.9 ± 2.2
609 ± 10
7.6 ± 2.8
100 μm
U–Pb age (2σ)
ε_{Hf(t)} (2σ)
(h) UD 34
587 ± 9
2686 ± 40
665 ± 9
(i) UD 35
629 ± 10
667 ± 11
-6.8 ± 2.8
575 ± 10
-5.1 ± 2.7
-7.3 ± 2.0
(j) UD 11
6.7 ± 3.4
1193 ± 18
1306 ± 18
0.8 ± 2.2
1357 ± 15
6.0 ± 2.0
(k) UD 20
0.1 ± 1.5
2087 ± 12
-6.4 ± 2.2
-8.5 ± 1.6
597 ± 18
0.2 ± 2.0
573 ± 18

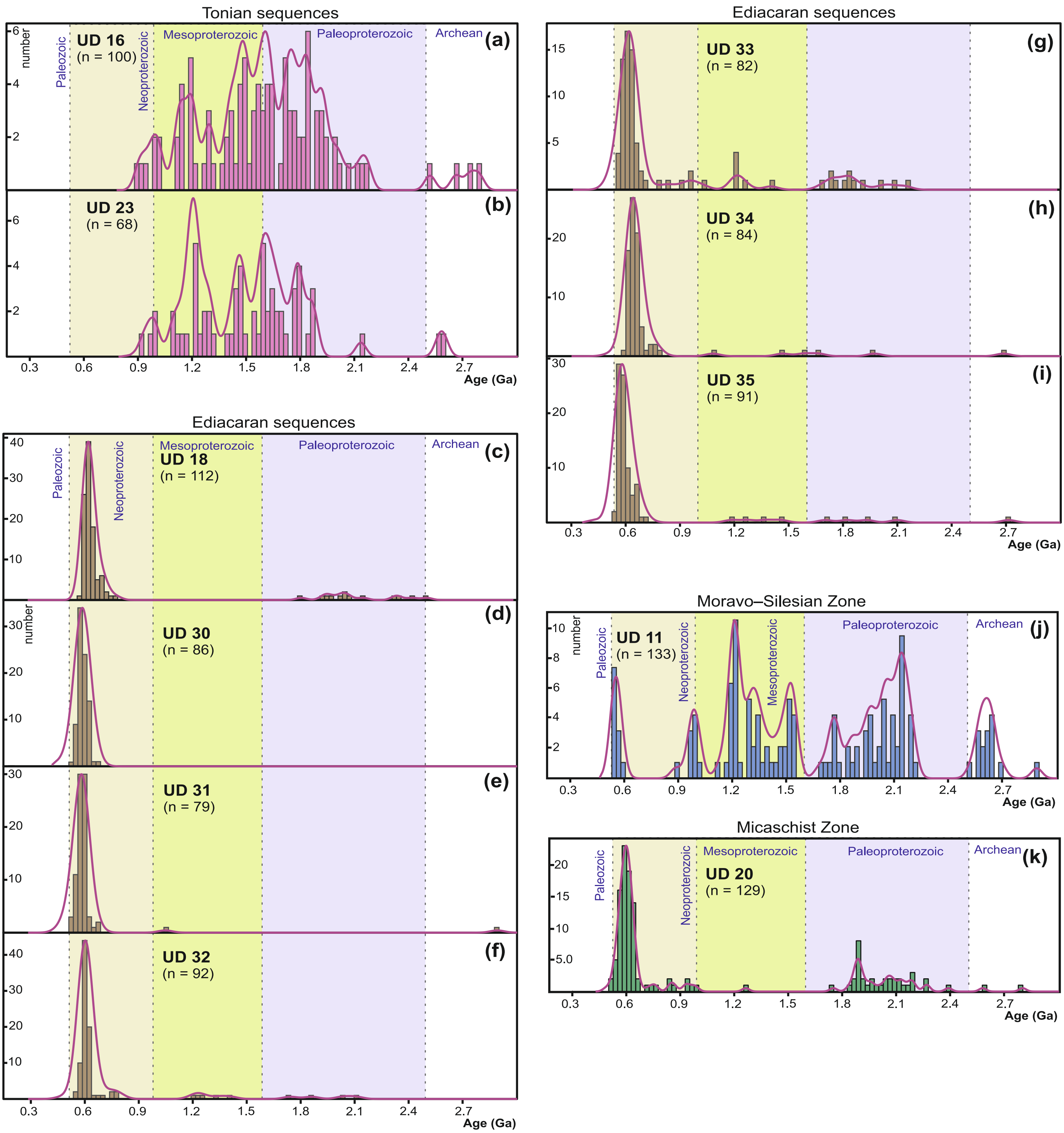
Tonian sequences
UD 16
(n = 100)
(a)
UD 23
(n = 68)
(b)
Ediacaran sequences
UD 18
(n = 112)
(c)
UD 30
(n = 86)
(d)
UD 31
(n = 79)
(e)
UD 32
(n = 92)
(f)
Ediacaran sequences
UD 33
(n = 82)
(g)
UD 34
(n = 84)
(h)
UD 35
(n = 91)
(i)
Moravo–Silesian Zone
UD 11
(n = 133)
(j)
Micaschist Zone
UD 20
(n = 129)
(k)
Paleozoic
Neoproterozoic
Mesoproterozoic
Paleoproterozoic
Archean
number
Age (Ga)
0.3
0.6
0.9
1.2
1.5
1.8
2.1
2.4
2.7

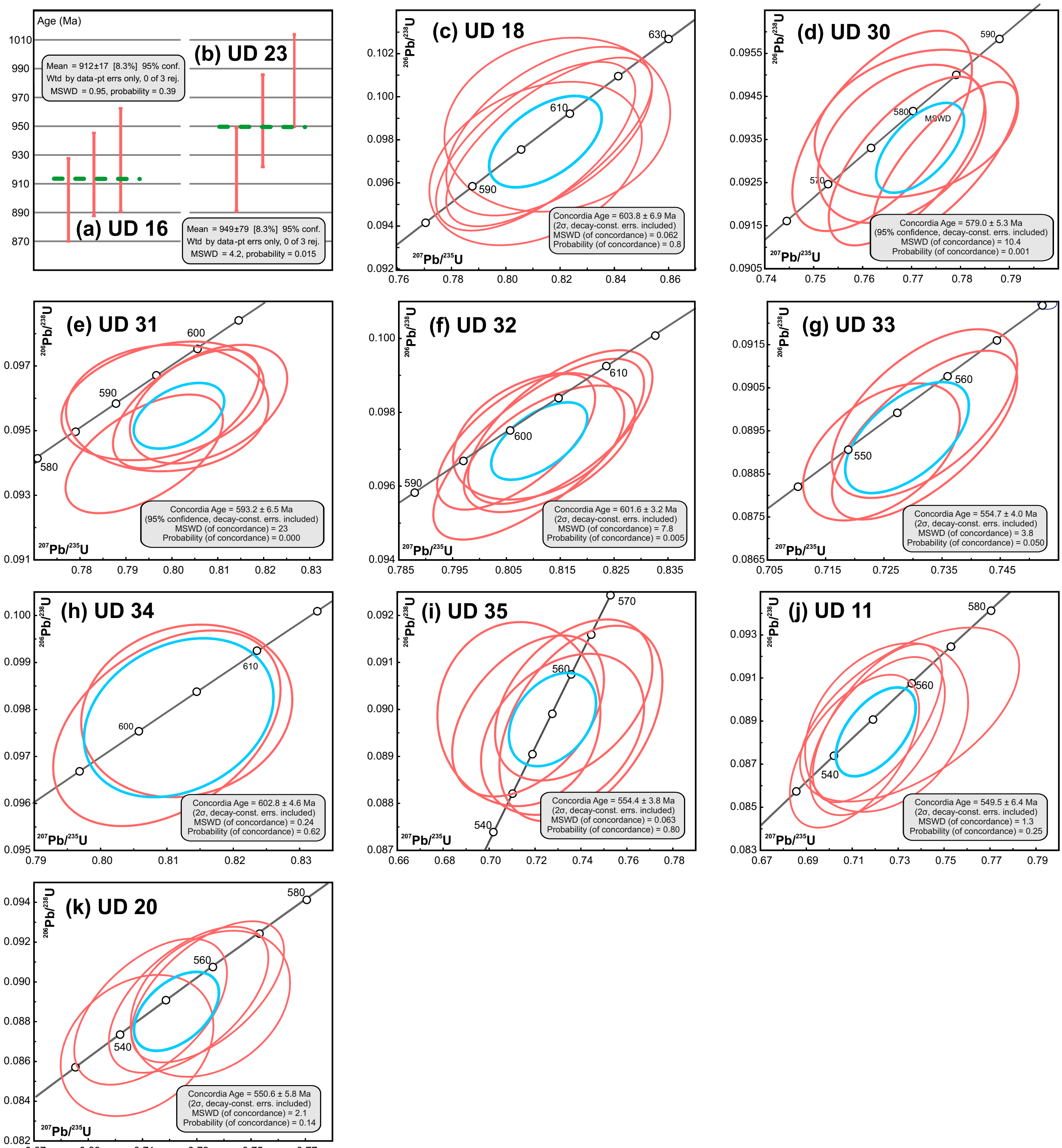

Age (Ma)
Mean = 912±17 [8.3%] 95% conf.
Wtd by data-pt errs only, 0 of 3 rej.
MSWD = 0.95, probability = 0.39
(a) UD 16
(b) UD 23
Mean = 949±79 [8.3%] 95% conf.
Wtd by data-pt errs only, 0 of 3 rej.
MSWD = 4.2, probability = 0.015
(c) UD 18
Concordia Age = 603.8 ± 6.9 Ma
(2σ, decay-const. errs. included)
MSWD (of concordance) = 0.062
Probability (of concordance) = 0.8
(d) UD 30
Concordia Age = 579.0 ± 5.3 Ma
(95% confidence, decay-const. errs. included)
MSWD (of concordance) = 10.4
Probability (of concordance) = 0.001
(e) UD 31
Concordia Age = 593.2 ± 6.5 Ma
(95% confidence, decay-const. errs. included)
MSWD (of concordance) = 23
Probability (of concordance) = 0.000
(f) UD 32
Concordia Age = 601.6 ± 3.2 Ma
(2σ, decay-const. errs. included)
MSWD (of concordance) = 7.8
Probability (of concordance) = 0.005
(g) UD 33
Concordia Age = 554.7 ± 4.0 Ma
(2σ, decay-const. errs. included)
MSWD (of concordance) = 3.8
Probability (of concordance) = 0.050
(h) UD 34
Concordia Age = 602.8 ± 4.6 Ma
(2σ, decay-const. errs. included)
MSWD (of concordance) = 0.24
Probability (of concordance) = 0.62
(i) UD 35
Concordia Age = 554.4 ± 3.8 Ma
(2σ, decay-const. errs. included)
MSWD (of concordance) = 0.063
Probability (of concordance) = 0.80
(j) UD 11
Concordia Age = 549.5 ± 6.4 Ma
(2σ, decay-const. errs. included)
MSWD (of concordance) = 1.3
Probability (of concordance) = 0.25
(k) UD 20
Concordia Age = 550.6 ± 5.8 Ma
(2σ, decay-const. errs. included)
MSWD (of concordance) = 2.1
Probability (of concordance) = 0.14
206Pb/238U
207Pb/235U

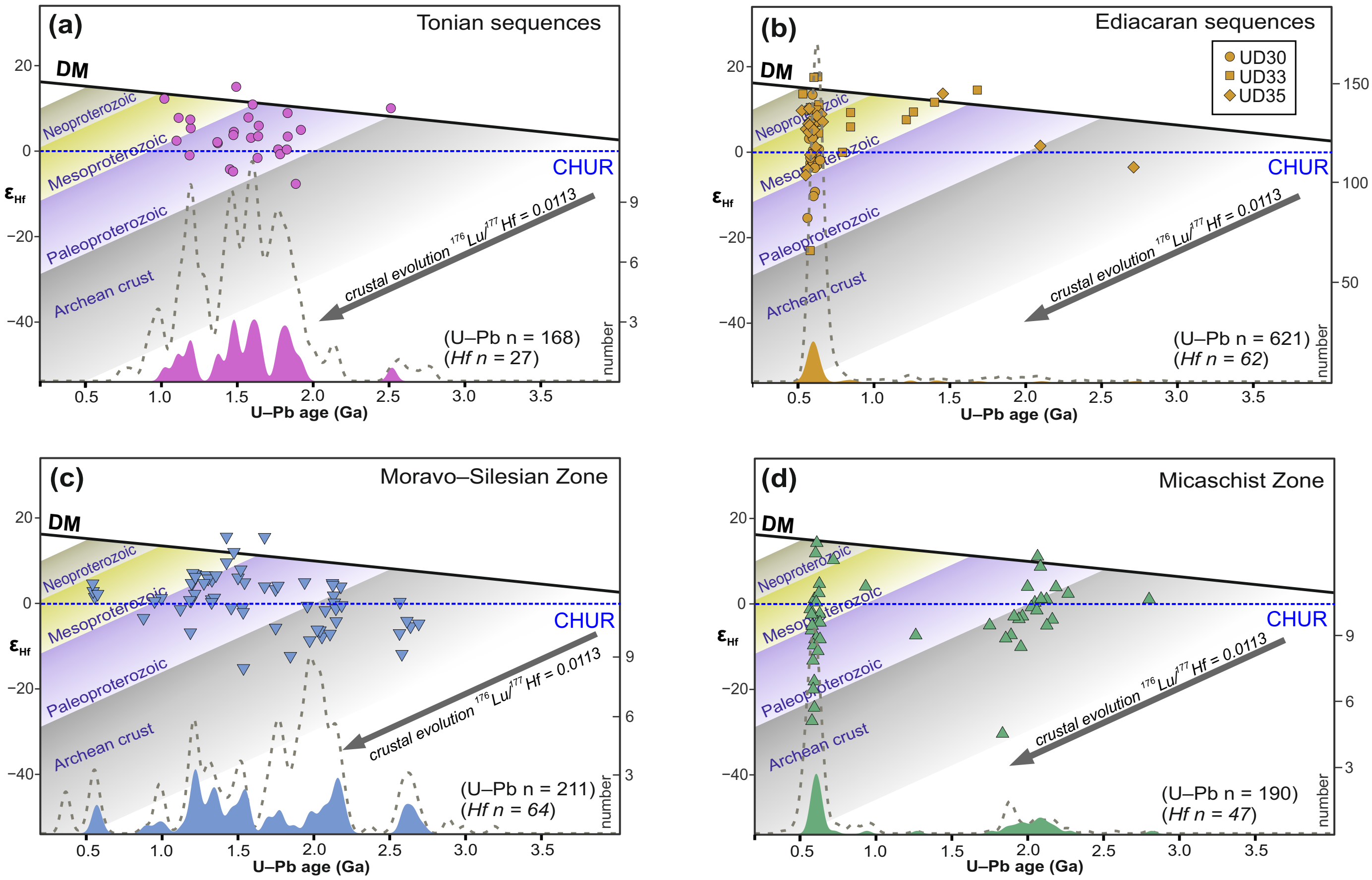
(a)
Tonian sequences
DM
Neoproterozoic
Mesoproterozoic
Paleoproterozoic
Archean crust
CHUR
crustal evolution 176Lu/177Hf = 0.0113
(U–Pb n = 168)
(Hf n = 27)
U–Pb age (Ga)
number
(b)
Ediacaran sequences
UD30
UD33
UD35
(U–Pb n = 621)
(Hf n = 62)
(c)
Moravo–Silesian Zone
(U–Pb n = 211)
(Hf n = 64)
(d)
Micaschist Zone
(U–Pb n = 190)
(Hf n = 47)

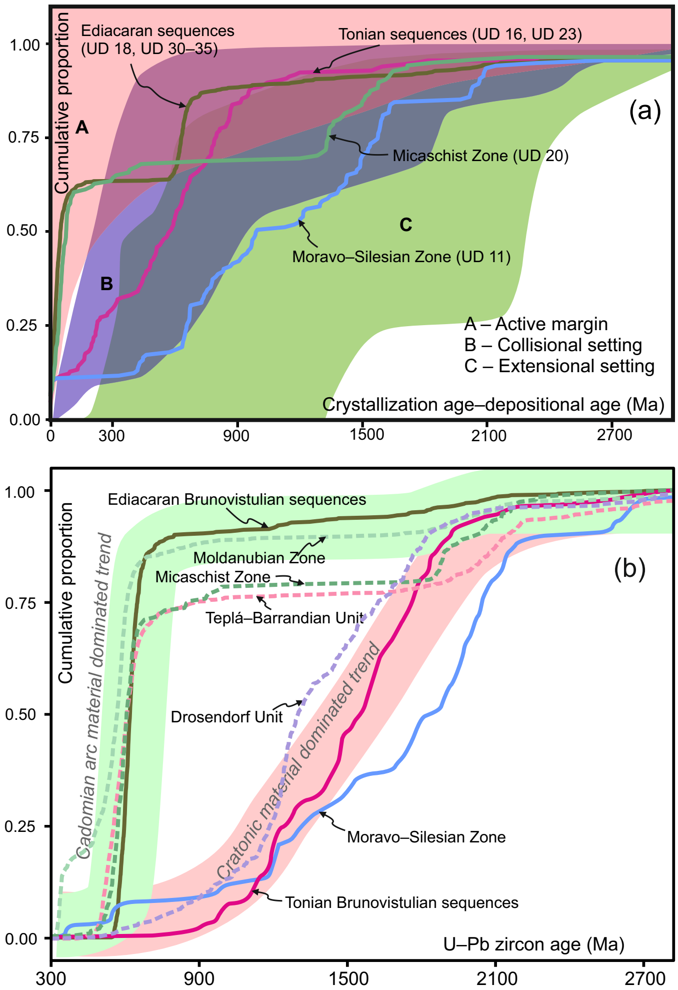

Ediacaran sequences
(UD 18, UD 30–35)
Tonian sequences (UD 16, UD 23)
Cumulative proportion
A
B
C
(a)
Micaschist Zone (UD 20)
Moravo–Silesian Zone (UD 11)
A – Active margin
B – Collisional setting
C – Extensional setting
Crystallization age–depositional age (Ma)
1.00
0.75
0.50
0.25
0.00
0
300
900
1500
2100
2700
Ediacaran Brunovistulian sequences
Moldanubian Zone
Micaschist Zone
Teplá–Barrandian Unit
Drosendorf Unit
Cadomian arc material dominated trend
Cratonic material dominated trend
Moravo–Silesian Zone
Tonian Brunovistulian sequences
U–Pb zircon age (Ma)
(b)

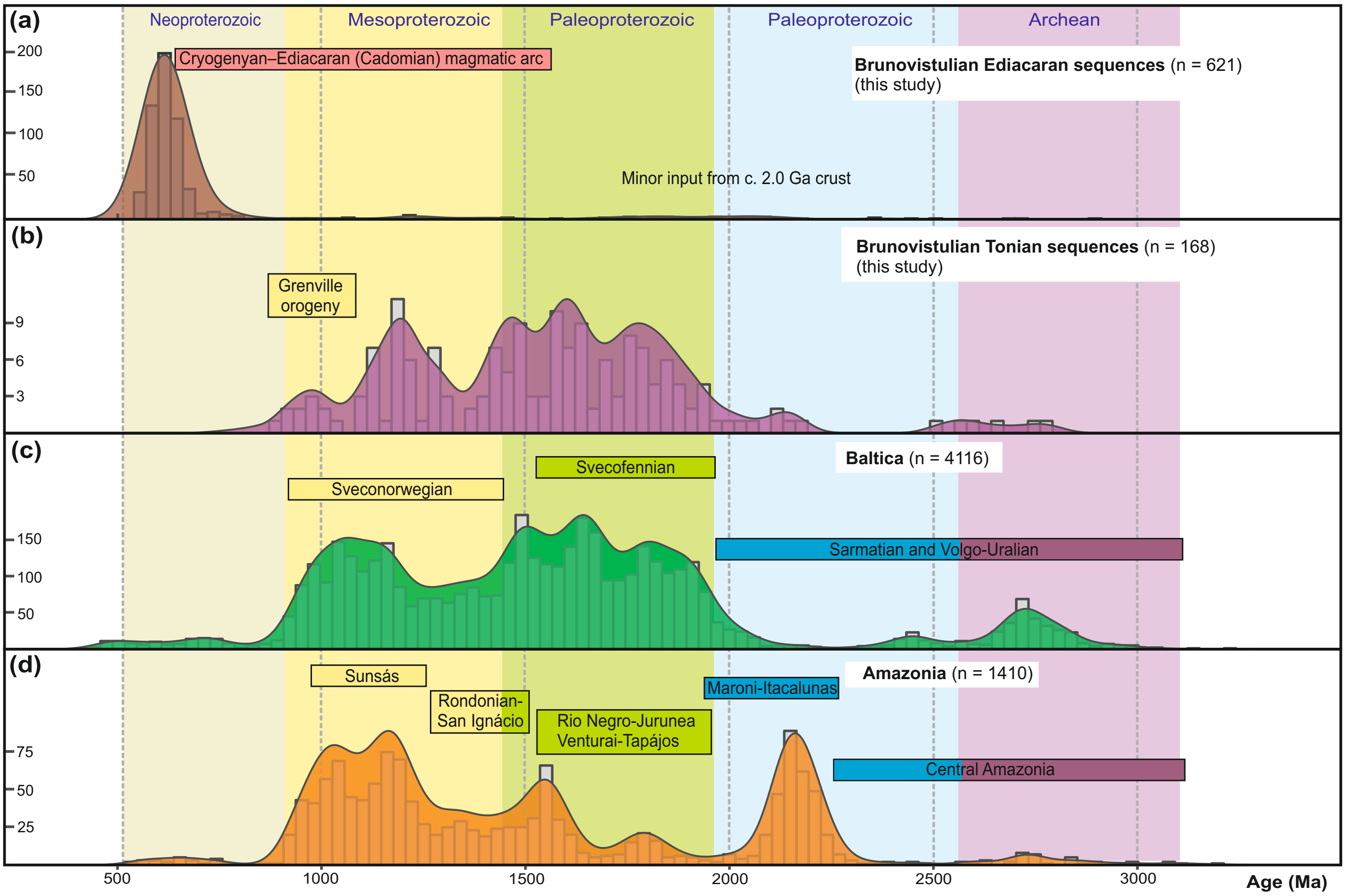

(a)
Neoproterozoic
Mesoproterozoic
Paleoproterozoic
Paleoproterozoic
Archean
200
150
100
50
Cryogenyan–Ediacaran (Cadomian) magmatic arc
Brunovistulian Ediacaran sequences (n = 621)
(this study)
Minor input from c. 2.0 Ga crust
(b)
Brunovistulian Tonian sequences (n = 168)
(this study)
Grenville
orogeny
9
6
3
(c)
Baltica (n = 4116)
Svecofennian
Sveconorwegian
150
100
50
Sarmatian and Volgo-Uralian
(d)
Amazonia (n = 1410)
Sunsás
Rondonian-
San Ignácio
Maroni-Itacalunas
Rio Negro-Jurunea
Venturai-Tapájos
75
50
25
Central Amazonia
500
1000
1500
2000
2500
3000
Age (Ma)

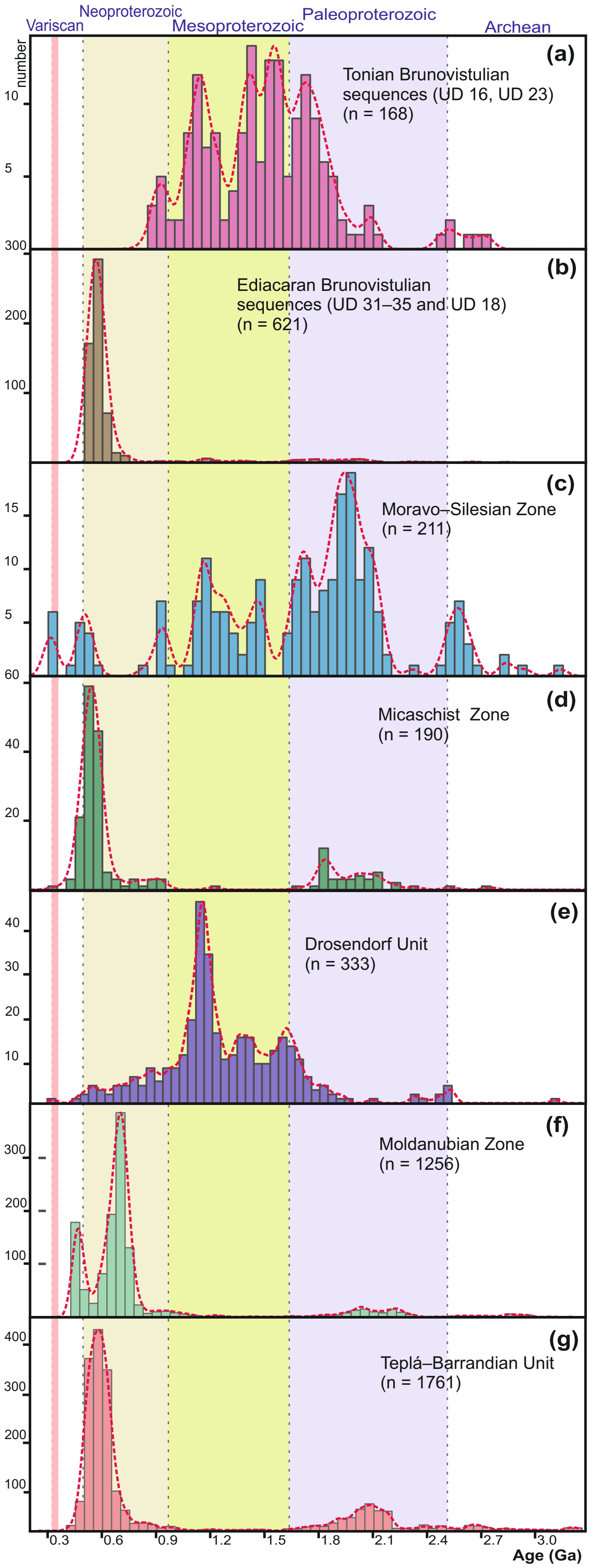

Variscan
Neoproterozoic
Mesoproterozoic
Paleoproterozoic
Archean
number
(a)
Tonian Brunovistulian sequences (UD 16, UD 23) (n = 168)
(b)
Ediacaran Brunovistulian sequences (UD 31–35 and UD 18) (n = 621)
(c)
Moravo–Silesian Zone (n = 211)
(d)
Micaschist Zone (n = 190)
(e)
Drosendorf Unit (n = 333)
(f)
Moldanubian Zone (n = 1256)
(g)
Teplá–Barrandian Unit (n = 1761)
0.3
0.6
0.9
1.2
1.5
1.8
2.1
2.4
2.7
3.0
Age (Ga)

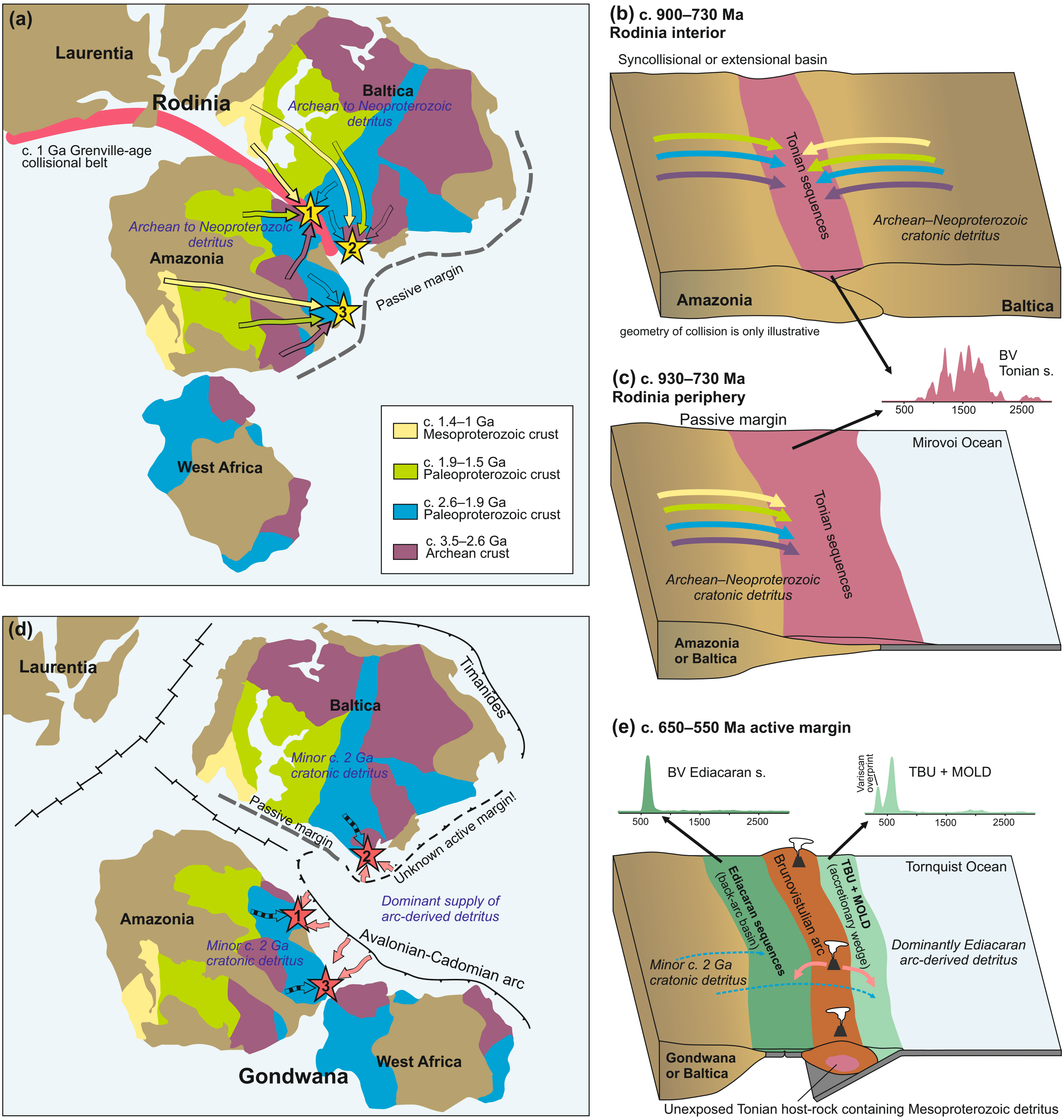
(a)
Laurentia
Rodinia
c. 1 Ga Grenville-age collisional belt
Baltica
Archean to Neoproterozoic detritus
Archean to Neoproterozoic detritus
Amazonia
Passive margin
West Africa
c. 1.4–1 Ga Mesoproterozoic crust
c. 1.9–1.5 Ga Paleoproterozoic crust
c. 2.6–1.9 Ga Paleoproterozoic crust
c. 3.5–2.6 Ga Archean crust
(b) c. 900–730 Ma
Rodinia interior
Syncollisional or extensional basin
Tonian sequences
Archean–Neoproterozoic cratonic detritus
Amazonia
Baltica
geometry of collision is only illustrative
BV Tonian s.
500 1500 2500
(c) c. 930–730 Ma
Rodinia periphery
Passive margin
Mirovoi Ocean
Tonian sequences
Archean–Neoproterozoic cratonic detritus
Amazonia or Baltica
(d)
Laurentia
Baltica
Timanides
Minor c. 2 Ga cratonic detritus
Passive margin
Unknown active margin!
Dominant supply of arc-derived detritus
Amazonia
Minor c. 2 Ga cratonic detritus
Avalonian-Cadomian arc
West Africa
Gondwana
(e) c. 650–550 Ma active margin
BV Ediacaran s.
500 1500 2500
Variscan overprint
TBU + MOLD
500 1500 2500
Tornquist Ocean
Ediacaran sequences (back-arc basin)
Brunovistulian arc
TBU + MOLD (accretionary wedge)
Minor c. 2 Ga cratonic detritus
Dominantly Ediacaran arc-derived detritus
Gondwana or Baltica
Unexposed Tonian host-rock containing Mesoproterozoic detritus